Geol. Mag. **132** (2), *1995, pp. 151–170.*

Compressional and extensional tectonics in low–medium pressure granulites from the Larsemann Hills, East Antarctica

C. J. CARSON*[1], P. G. H. M. DIRKS†[2], M. HAND*[3], J. P. SIMS* & C. J. L. WILSON*

* School of Earth Sciences, University of Melbourne, Parkville, 3052, Australia
† Institute of Earth Sciences, University of Utrecht, The Netherlands

(*Received* 2 December 1993; *revised version received* 29 August 1994; *accepted* 2 November 1994)

Abstract – Meta-sediments in the Larsemann Hills that preserve a coherent stratigraphy, form a cover sequence deposited upon basement of mafic–felsic granulite. Their outcrop pattern defines a 10 kilometre wide east–west trending synclinal trough structure in which basement–cover contacts differ in the north and the south, suggesting tectonic interleaving during a prograde, D_1, thickening event. Subsequent conditions reached low–medium pressure granulite grade, and structures can be divided into two groups, D_2 and D_3, each defined by a unique lineation direction and shear sense. D_2 structures which are associated with the dominant gneissic foliation in much of the Larsemann Hills, contain a moderately east-plunging lineation indicative of west-directed thrusting. D_2 comprises a co-linear fold sequence that evolved from early intrafolial folds to late upright folds. D_3 structures are associated with a high-strain zone, to the south of the Larsemann Hills, where S_3 is the dominant gneissic layering and folds sequences resemble D_2 folding. Outside the D_3 high-strain zone occurs a low-strain D_3 window, preserving low-strain D_3 structures (minor shear bands and upright folds) that partly re-orient D_2 structures. All structures are truncated by a series of planar pegmatites and parallel D_4 mylonite zones, recording extensional dextral displacements.

D_2 assemblages include coexisting garnet–orthopyroxene pairs recording peak conditions of $\sim$ 7 kbar and $\sim$ 780 °C. Subsequent retrograde decompression textures partly evolved during both D_2 and D_3 when conditions of $\sim$ 4–5 kbar and $\sim$ 750 °C were attained. This is followed by D_4 shear zones which formed around 3 kbar and $\sim$ 550 °C.

It is tempting to combine D_{2-4} structures in one tectonic cycle involving prograde thrusting and thickening followed by retrograde extension and uplift. The available geochronological data, however, present a number of interpretations. For example, D_2 was possibly associated with a clockwise *P–T* path at medium pressures around $\sim$ 1000 Ma, by correlation with similar structures developed in the Rauer Group, whilst D_3 and D_4 events occurred in response to extension and heating at low pressures at $\sim$ 550 Ma, associated with the emplacement of numerous granitoid bodies. Thus, decompression textures typical for the Larsemann Hills granulites maybe the combined effect of two separate events.

1. Introduction

The Larsemann Hills, located on the Ingrid Christensen Coast of Prydz Bay, East Antarctica (Fig. 1), consist of a number of small ice-free peninsulas and off-shore islands representing some 60 km^2 of exposure. The area is dominated by migmatitic pelitic, psammitic and felsic paragneisses which are extensively intruded by peraluminous granitic and pegmatitic bodies (Stüwe, Braun & Peer, 1989; Dirks, Carson & Wilson, 1993). This region forms part of the extensive high-grade metamorphic complex of East Antarctica, which is generally interpreted to have evolved during one Neoproterozoic ($\sim$ 1000 Ma) granulite facies event (see, e.g. Tingey, 1981; Black *et al.* 1987; Stüwe, Braun & Peer, 1989). Within the Prydz Bay area, post-peak metamorphic textures, indicative of decompression, have been used to infer a clockwise *P–T* path for this event (see, e.g. Harley, 1988; Stüwe & Powell, 1989*a*; Nichols & Berry, 1991; Harley & Fitzsimons, 1991; Fitzsimons & Harley, 1992).

The contribution of the Pan-African event ($\sim$ 550 Ma) to the structural and metamorphic evolution of the Larsemann Hills has become increasingly recognized. Zhao *et al.* (1992) report Pan-African ages for syn-deformational intrusives in the Larsemann Hills, which led Ren *et al.* (1992) to conclude that the pervasive structural and *P–T* evolution of the area is of Pan-African age. Dirks, Carson & Wilson (1993) alternatively suggest that the observed decompression textures in the Larsemann Hills, rather than being the result of a continuous clockwise *P–T* evolution during

[1] Corresponding author.
[2] Present address: Dept. of Geology, University of Zimbabwe, P.O. Box MP167, Harare, Zimbabwe.
[3] Present address: Dept. of Geology and Geophysics, Adelaide University, Adelaide, S.A. 5005, Australia.

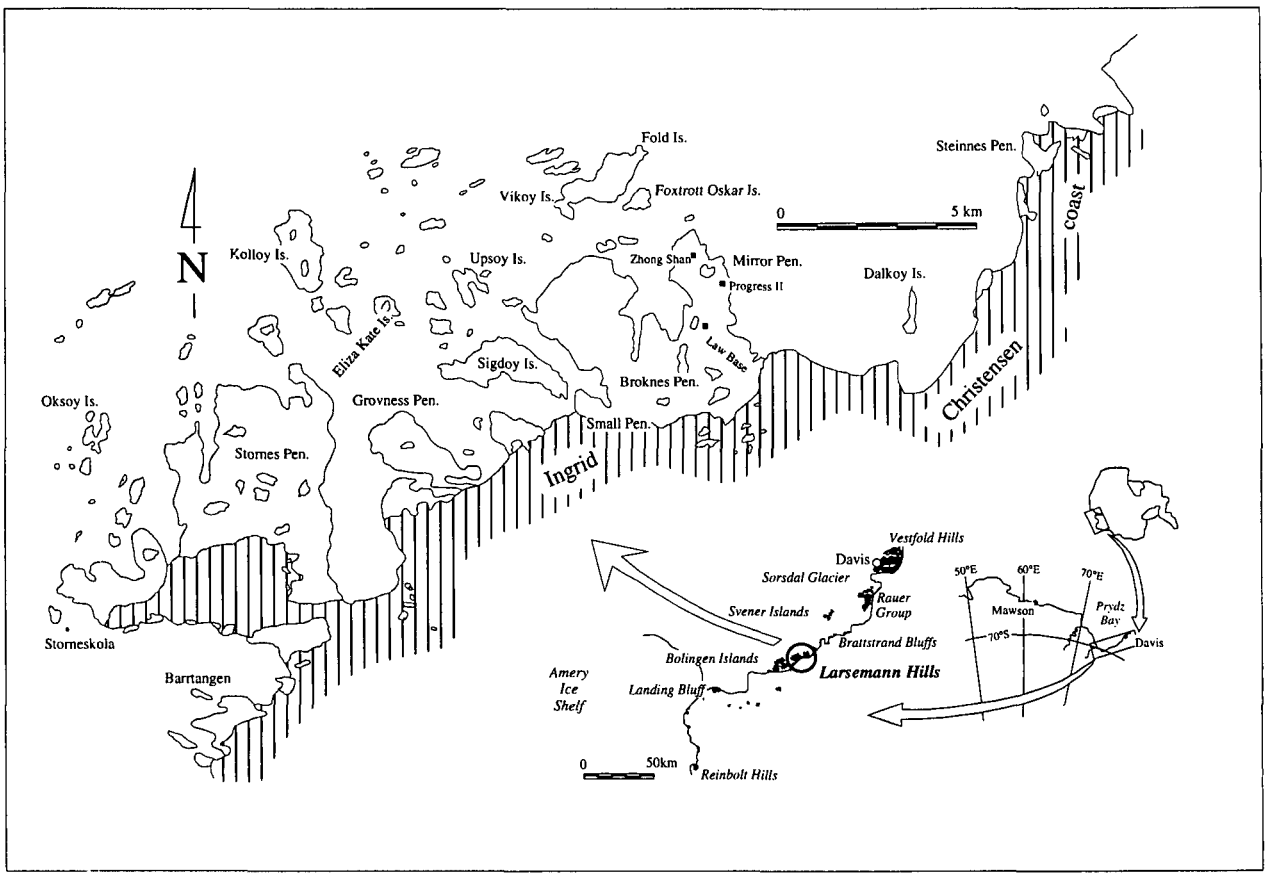

Figure 1. Map of the Larsemann Hills region. Original names after Stüwe, Braun & Peer (1989) have been retained. Inset shows location of Larsemann Hills within the Prydz Bay area.

either a single 1000 Ma or 550 Ma event, may instead be the result of superposition of two unrelated metamorphic peaks (one at ~ 1000 Ma, post-dated by a second at lower pressure at ~ 550 Ma).

In this paper, we present stratigraphic, structural and kinematic data relevant to the Larsemann Hills, expanding on the earlier structural analyses of Stüwe, Braun & Peer (1989) and Dirks, Carson & Wilson (1993). Relevant micro-textures, recent geochronology and kinematics are integrated within this expanded structural framework. Discussion will focus on the relative effects of the Neoproterozoic (~ 1000 Ma) event and the Pan-African (~ 550 Ma) event in the Larsemann Hills in the light of this information.

2. Lithologies

The Larsemann Hills (including Steinnes Peninsula, Fig. 1) consist predominantly of upper amphibolite to granulite grade paragneisses intruded by numerous generations of pegmatitic and granitic bodies. The area forms part of a metasedimentary sequence which extends to at least the Bolingen Islands to the south (Dirks & Hand, 1995) and the Brattstrand Bluffs (Fitzsimons & Harley, 1991) and western Rauer Group to the north (Harley, 1987). Two primary associations can be identified: (i) a composite mafic–felsic orthogneiss, which forms the boundary of and is interleaved with a (ii) metasedimentary pile, which comprises the bulk of the outcrop in the Larsemann Hills (Figs 2, 3). Figure 4 shows a comparison of previous workers lithological descriptions with that presented here.

2.a. Basement

'Composite orthogneiss' crops out on Barrtangen and Steinnes Peninsula and on northern offshore islands (e.g. Kolloy, northeast Vikoy and Fold islands). The composite orthogneiss largely consists of felsic gneiss with discontinuous pods, boudins and layers of mafic units that generally comprise around 10–20%, but locally up to 80–90% of the total rock volume.

The host orthogneiss is homogeneous, light-brown, medium-grained (0.5–2.0 mm) and composed of quartz, feldspar, biotite ± orthopyroxene in southern outcrops, but is more trondhjemitic on northern offshore islands. The mafic component is dominated by hornblende–orthopyroxene assemblages with variable amounts of clinopyroxene, biotite, plagioclase ± quartz that are commonly truncated by felsic leucosomes with minor orthopyroxene–biotite ± clinopyroxene. Rare calc-silicate boudin trains are present

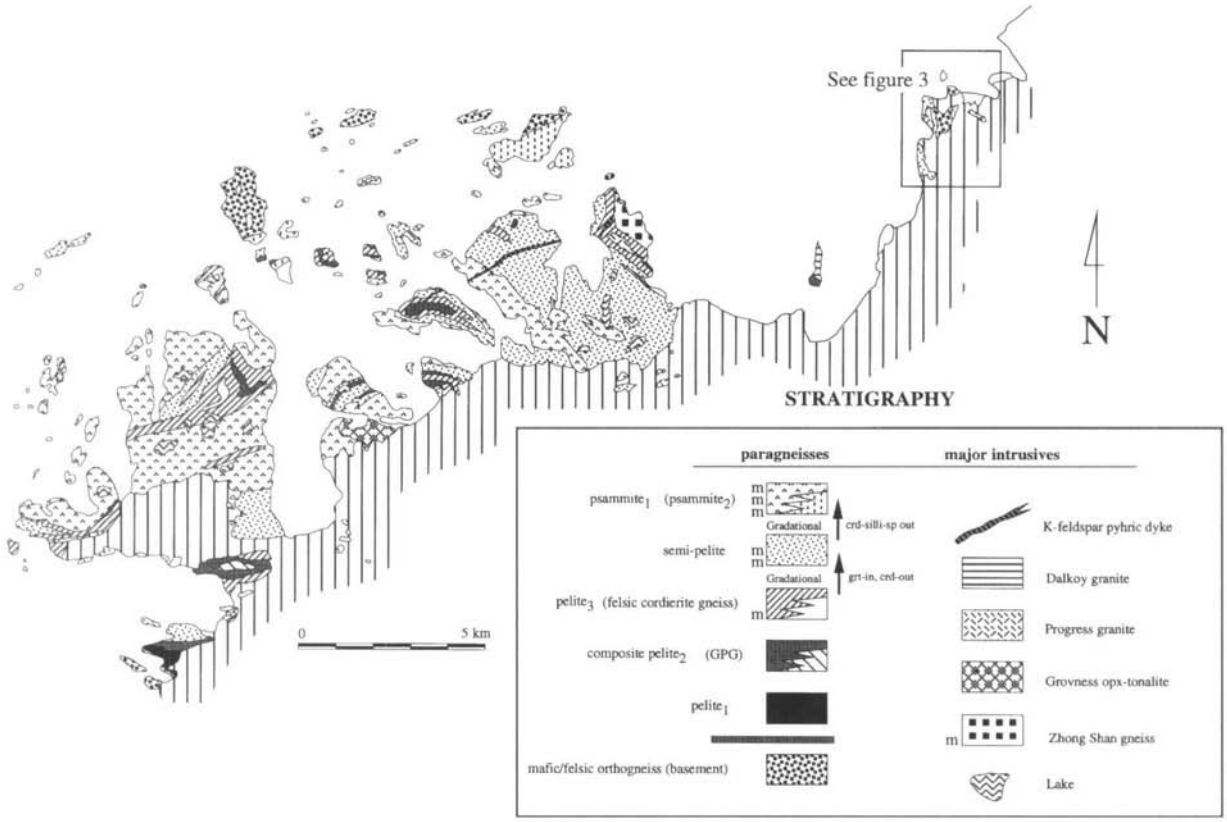

Figure 2. Lithological map of the Larsemann Hills, with inferred stratigraphic column for meta-sedimentary units. Major intrusive lithologies are listed in order of degree of deformation. 'm' represents presence of metabasite bodies in relevant units.

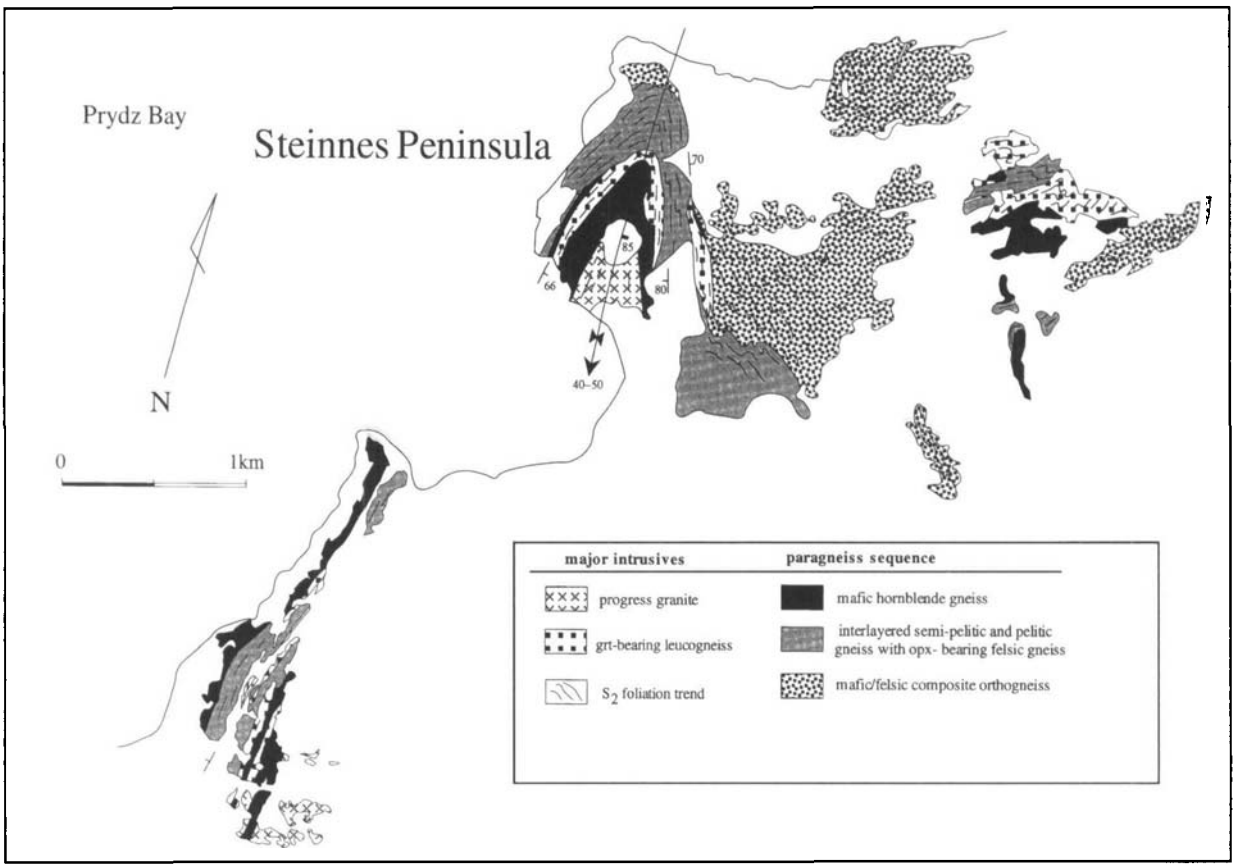

Figure 3. Lithological map of Steinnes Peninsula. Major south-plunging F_3^{lsz} structure is shown, the synonymous of F_4 of Fitzsimons & Harley (1991). The dominant foliation present is S_2.

This paper	Stüwe, Braun & Peer, 1989	Dirks *et al.* 1993	Ren *et al.* 1992	Zhao *et al.* 1992	Fitzsimons & Harley, 1991
		Paragneiss sequence			Brattstrand Bluffs
psammite$_1$			felsic gneiss		
psammite$_2$	layered gneiss				
semi-pelite	yellow gneiss	migmatitic paragneiss	migmatitic gneiss	striped migmatite	? semi-pelite$_{i\ \&\ ii}$?
pelite$_3$ felsic cordierite gneiss	white gneiss				
composite pelite$_2$ granular porhyroblastic gneiss	blue gneiss	cordierite-spinel gneiss	? magnetite-cordierite-heterogenous gneiss ?	? high Al-Fe gneiss ?	? metapelite ?
pelite$_1$					
		basement			
composite orthogneiss	pyroxene bearing gneiss		banded gneiss	two pyroxene gneiss	composite orthogneiss
		major intrusive units			
Dalkoy granite	grey granite	granitic gneiss VI			Dalkoy granite
Zhong Shan gneiss	painted gneiss	granitic gneiss I	leucogneiss	gneissic leucocratic-granite	leucogneiss ?
Progress granite	pink granite	granitic gneiss V	syenitic orthogneiss	syenogranite	GOG (granitic orthogneiss)
Grovness opx-tonalite					
augen K-feldspar orthogneiss$_1$					
porphyroblastic K-feldspar orthogneiss$_2$					

Figure 4. Correlative framework for the major lithological units proposed for the Larsemann Hills area. Intrusive units only refer to the major igneous bodies discussed in the text. '?' indicates uncertainty of the proposed correlation. The 'blue gneiss' of Stüwe, Braun & Peer (1989) represents one sub-division of the composite pelite$_2$ proposed here.

as narrow (1 m) layers within the composite orthogneiss (e.g. Barrtangen).

2.b. Metasediments

The inferred cover sequence consists of alternating aluminous pelites that grade to more psammitic and felsic units. The constituent units are described in the order they occur, from the contact with the basement orthogneiss in the southeast Larsemann Hills (Fig. 2). As there are no sedimentary younging criteria observed within the sequence, the presented order should not be strictly interpreted as a progressively younging sequence. The description of lithologies and lithological stratigraphy presented here differs from that of previous workers (e.g. Sheraton, Black & McCulloch, 1984; Stüwe, Braun & Peer, 1989; Dirks, Carson & Wilson, 1993) and several additional lithological units are described.

2.b.1. Pelite$_1$

This unit constitutes around 10% of the outcrop in the Larsemann Hills, and is generally present as continuous layers of variable thickness (~ 10–400 m). No metabasite layers or pods are present within this unit. Pelite$_1$ is characterized by a wispy, 'rope-like' appearance produced by bundles of coarse-grained sillimanite, spinel and magnetite interleaved with generally pink K-feldspar-rich leucosomes (up to 10 mm wide) that locally account for 75–85% of the unit. Cordierite is common in the sillimanite–spinel domains, but restricted to the margins of the K-feldspar leucosomes. The nature of the contact with the mafic–felsic orthogneiss is obscured, however, the contact with the overlying composite pelite$_2$ is generally sharp.

2.b.2. Composite pelite$_2$

This composite unit, which comprises around 10% of exposure, consists of a number of rock types that are interbedded on a metric scale. It varies in thickness from narrow (20–50 m wide) occurrences at Barrtangen, to larger bodies (up to 100 m) on central Stornes Peninsula and Sigdoy Island (Figs 1, 2). Composite pelite$_2$ comprises the following units:

(i) A discontinuous coarse-grained, cordierite-dominated, spinel–sillimanite–biotite–ilmenite–magnetite gneiss with highly variable amounts of coarse subhedral garnet, K-feldspar and quartz ('blue gneiss' of Stüwe, Braun & Peer, 1989). Cordierite forms an extensive multigrained matrix in which all other phases are present. Cordierite also forms inclusion-free coronas on garnet (Stüwe & Powell, 1989*a*). Massive pods of coarse-grained cordierite–biotite and euhedral spinel–magnetite are common.

(ii) Megacrystic orthopyroxene-bearing tonalite (±biotite and garnet) occurs as narrow layers and lenses up to 50 cm wide, and is comprised of equidimensional plagioclase–quartz–biotite matrix host large blasts of euhedral orthopyroxene (up to 30 mm diameter, see Stüwe & Powell, 1989*b*, fig. 1c). Orthopyroxene blasts may have a 'spongy' appearance due to numerous inclusions of quartz, and are variably mantled by coarse biotite.

(iii) Sulphide-rich quartzite occurs as narrow (4–5 m), laterally discontinous layers and forms characteristic dark yellow and iron-oxide stained gossan-like outcrops with coarse skeletal cubic limonite (after pyrite?) and numerous patches of secondary anhedral azurite and malachite. Associated coarse-grained blue quartzite layers and pods are also common.

(iv) A distinctive, homogeneous, medium grained ($\sim$ 1 mm), light grey, plagioclase–biotite–spinel $\pm$ magnetite $\pm$ quartz gneiss, the 'granular-porphyroblastic-gneiss' (GPG sub-unit), occurs as lensoid, discontinuous pods up to 200 m long and several tens of metres wide. This sub-unit characteristically hosts large (up to 30 mm diameter), euhedral Fe–Mg porphyroblasts that typically consist of a single unzoned almandine garnet or cordierite blast, which are mantled by coarse plagioclase (cf. Stüwe & Powell, 1989*b*). Inclusions within the blasts are generally coarse biotite, plagioclase feldspar, ilmenite and magnetite, which may or may not be aligned with the external foliation. Multi-minerallic aggregates are also present within this sub-unit. These are composed of a aggregate core with variable amounts of garnet–cordierite–kornerupine–spinel–biotite–grandidierite, again variably mantled by plagioclase (Carson, Hand & Dirks, 1995; Ren *et al.* 1992). Such blasts and multi-minerallic aggregates generally cross-cut the host biotite foliation, but locally they can be flattened within and tightly to isoclinally folded by that foliation.

2.b.3. Pelite$_3$

Pelite$_3$ is similar to pelite$_1$ but it is garnet-bearing. It locally contains a very leucocratic quartz–plagioclase–K-feldspar–cordierite sub-unit ('felsic cordierite gneiss' = 'white gneiss', Stüwe, Braun & Peer, 1989) which is rarely garnetiferous with distinctive cordierite–quartz symplectites. This unit is particularly common on central and eastern Stornes Peninsula. Metabasite pods and layers consisting of predominantly hornblende–plagioclase–biotite $\pm$ orthopyroxene are present, but are uncommon.

2.b.4. Semi-pelite

This unit accounts for up to 40% of the total outcrop in the Larsemann Hills, and up to 80% of outcrop on Broknes Peninsula (Fig. 2). Semi-pelite is a heterogeneous fine- to medium-grained garnet–sillimanite–spinel–plagioclase–quartz $\pm$ biotite gneiss with a characteristic sugary texture and a yellow to pale weathering colouration. The modal amounts of spinel and sillimanite are highly variable and cordierite is uncommon. Magnetite forms coarse (20–30 mm diameter) euhedral segregations. Semi-pelite has a transitional contact with pelite$_3$, with garnet becoming more abundant at the expense of cordierite (Fig. 2). A common feature of this unit is the occurrence of discontinuous hornblende, orthopyroxene, clinopyroxene, biotite, plagioclase-bearing mafic lenses and boudin pods($\sim$ 5% of the unit). This unit is equivalent to the 'yellow gneiss' of Stüwe, Braun & Peer (1989); 'migmatitic paragneiss' of Dirks, Carson & Wilson (1993) and 'striped migmatite' of Zhao *et al.* (1992).

2.b.5. Psammite$_1$

This unit accounts for $\sim$ 40% of the total outcrop and up to 70% of outcrop on Stornes Peninsula (Fig. 2). It generally forms a homogeneous unit with equigranular granitic appearance, with quartz, plagioclase, K-feldspar and variable amounts of garnet and biotite. Sillimanite is rare and cordierite is absent. Small aluminous enclaves ($\sim$ 10–20 cm diameter) are composed of coarse-grained sillimanite–spinel $\pm$ magnetite and minor cordierite can also be present. This unit is highly migmatized with up to three overprinting generations of garnet-bearing felsic leucosomes that cross-cut the primary compositional layering. Numerous metabasite pods and lenses are present (up to 5 m wide), dominated by hornblende–plagioclase assemblages with minor, variable, amounts of orthopyroxene, biotite and, ocassionally, clinopyroxene. Narrow, laterally extensive layers (30–40 cm wide) of coarse-grained radiating sprays of kornerupine are present. Rare garnet, orthopyroxene, plagioclase-bearing metabasite assemblages are also present. Psammite$_1$ is gradational with semi-pelite with cordierite, spinel and sillimanite becoming gradually less common.

2.b.6. Psammite$_2$

This felsic unit constitutes around 10% of total outcrop and differs from psammite$_1$ in that it contains more felsic component relative to Fe–Mg phases and lacks small aluminous enclaves and mafic lenses. Sillimanite and cordierite are also absent. This unit is common along the contact with the basement orthogneiss on the northern offshore islands, but generally absent elsewhere.

2.c. Intrusives

The Larsemann Hills are intruded by various generations of granitic and pegmatitic bodies (Fig. 2). Pegmatites and migmatitic bodies have developed synchronously and, less commonly, post-dating regional high grade deformation. The intrusive bodies have been interpreted as locally derived melts based on S-type geochemical signatures (Stüwe, Braun & Peer, 1989; Zhao *et al.* 1992). Dirks, Carson & Wilson (1993) described a detailed history of pegmatite intrusions, and these will not be discussed further.

2.c.1. Zhong Shan gneiss

This massive leucocratic quartzo-feldspathic gneiss 'painted rock' – Stüwe, Braun & Peer, 1989; 'granitic gneiss I' – Dirks, Carson & Wilson, 1993; 'gneissic leucogranite' – Zhao *et al.* 1992), crops out on northeastern Broknes Peninsula and preserves a clear foliation defined by stringers of garnet, rare biotite and a compositional banding defined by quartz–feldspar leucosomes. Hornblende–plagioclase-bearing metabasite units are present as isoclinally folded layers (Dirks, Carson & Wilson, 1993). On Steinnes Peninsula, this unit occurs as a strongly-foliated, narrow transposed layer (3–4 m wide). The primary nature of the Zhong Shan gneiss is unclear, but previous workers assumed an igneous origin based on its homogeneous nature (Stüwe, Braun & Peer, 1989; Dirks, Carson & Wilson, 1993), however, a sedimentary origin cannot be discounted. Zhao *et al.* (1992) determined a $^{207}Pb/^{206}Pb$ zircon age of 940 ± 6 Ma, and a Sm–Nd three point isochron (garnet + K-spar + whole rock) age of 497 ± 7 Ma for this rock.

2.c.2. Progress granite

A relatively large body of this granite outcrops on Mirror Peninsula ('granitic gneiss V' – Dirks, Carson & Wilson, 1993; 'pink granite' – Stüwe, Braun & Peer, 1989; 'syenogranite' – Zhao *et al.* 1992), with other minor occurrences on Steinnes Peninsula (Fig. 3; 'granitic orthogneiss', GOG – Fitzsimons & Harley, 1991), Barrtangen, Vikoy Island and various islands to the north of Upsoy Island (Fig. 2). It is comprised of medium- to coarse-grained K-feldspar and quartz with subordinate plagioclase. Biotite locally defines a weak to moderate foliation. Accessory phases include, in order of abundance, sub-anhedral garnet with rounded inclusions of quartz, magnetite, spinel, monazite and zircon. Zhao *et al.* (1992) determined a zircon $^{207}Pb/^{206}Pb$ age of 547 ± 9 Ma for the crystallization age of the Progress Granite from Mirror Peninsula.

2.c.3. Grovness Enderbite

A massive but well-foliated non-megacrystic orthopyroxene–tonalite body is exposed on southern Grovness Peninsula. It is dominated by medium-grained subhedral polygonal plagioclase and quartz with strongly corroded grains of orthopyroxene. Rare, strongly embayed, anhedral garnet, occurs both as isolated grains and in contact with orthopyroxene. Small euhedral magnetite grains (which occur on the rims of orthopyroxene grains), monazite, zircon and apatite are accessory phases. Subhedral biotite occurs as inclusions with orthopyroxene grains. An intrusive origin is preferred, based on the massive, extremely homogenous nature of this unit, but a sedimentary origin cannot be ruled out.

2.c.4. Dalkoy granite

The Dalkoy granite (Fitzsimons & Harley, 1991; 'granitic gneiss VI', Dirks, Carson & Wilson, 1993; 'grey granite', Stüwe, Braun & Peer, 1989) crops out on the northern portion of Dalkoy Island. It consists of medium-grained K-feldspar, quartz, plagioclase and biotite. K-feldspar and plagioclase are variably replaced by muscovite and sericite. Accessory phases include rounded magnetite grains, zircon, apatite and rare monazite. The unit contains a variably developed foliation defined by euhedral biotite and aligned quartz and feldspar. This foliation is axial planar to open folds defined by thin, discontinuous, quartzo-feldspathic leucosomes. The contact of the Dalkoy granite is concordant with the pervasive S_2 foliation of the host pelitic gneiss. The Dalkoy granite has been correlated with the Landing Bluff granitoid suite to the south by Stüwe, Braun & Peer (1989) and Fitzsimons & Harley (1991), for which a 493 ± 17 Ma age has been determined (Rb–Sr whole rock; Tingey, 1981).

2.c.5. Storneskola megacrystic K-feldspar orthogneiss units

Two porphyritic K-feldspar orthogneiss units occur as small isolated exposures on Storneskola (Fig. 1) and Stornes Peninsula regions, and account for less than 5% of total outcrop. Augen K-feldspar orthogneiss$_1$ is comprised of K-feldspar, plagioclase, quartz, biotite and minor garnet, with large (20–30 mm diameter) K-feldspar augen, which locally spectacularly define the ambient lineation (e.g. islands north of Storneskola). The augen K-feldspar orthogneiss$_1$ can occur in association with, and is clearly intruded by, the prophyroblastic K-feldspar orthogneiss$_2$, which consists of numerous large, euhedral, undeformed, K-feldspar porphyroblasts (20–70 mm long), within a finer ground-mass of K-feldspar, quartz, plagioclase, biotite (Fig. 5). Garnet occurs as subhedral grains within the ground-mass, and also occurs with coarse biotite as selvedges along the unit perimeter.

2.c.6. Late K-spar granitic dyke

A pink magnetite–sillimanite-bearing granitic dyke occurs on Broknes Peninsula and Sigdoy Island and has been described by Dirks, Carson & Wilson (1993) and Stüwe, Braun & Peer (1989). Zircon $^{207}Pb/^{206}Pb$ ages of 556 ± 7 Ma (sample ZG20405) have been obtained (Zhao *et al.* 1992).

2.d. Basement and cover relationships

Based on the lithological similarity with mafic–felsic orthogneiss from the southeastern Rauer Group and Berrneset Peninsula (Bolingen Island, Dirks & Hand, 1994) for which Archaean and Palaeoproterozoic formation ages (respectively) have been suggested

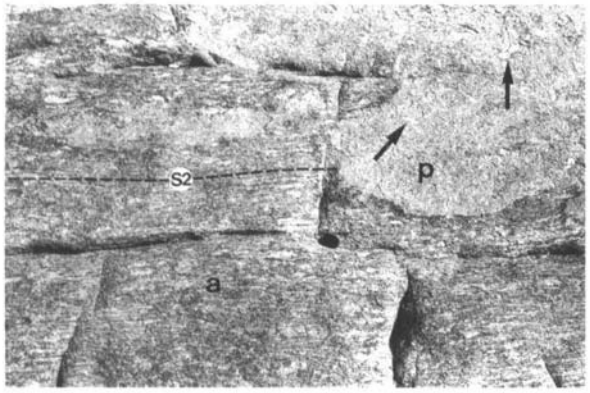

Figure 5. Augen K-feldspar orthogneiss$_1$ (labelled 'a', foliation is S_2) intruded by the porphyroblastic K-feldspar orthogneiss$_2$ (labelled 'p'), coarse unorientated phenocrysts of K-feldspar arrowed, Storneskola. Lens cap ~ 50 mm diameter.

(U–Pb – Black & Sheraton, 1993; Rb–Sr, sample 81285291 – Sheraton, Black & McCulloch, 1984), we assume that the mafic–felsic composite orthogneiss represents an archaean basement complex to the metasedimentary sequence of the Larsemann Hills. The extensive metasedimentary sequence, for which a range of Mesoproterzoic ages have been determined (1300–1600 Ma Rb–Sr ages – Sheraton, Black & McCulloch, 1984) is considered to have been derived from, and deposited on, the Archaean orthogneiss basement. Similar assumptions on the nature of the relationship between composite orthogneiss and paragneiss sequences is also assumed in the Brattstrand Bluffs and associated outcrops by Fitzsimons & Harley (1991, 1992) and the Bolingen Islands (Dirks & Hand, 1995). The primary nature of the orthogneiss–paragneiss contact is difficult to determine due to subsequent deformation and transposition. The nature of both the basement orthogneiss and its relationship with metasediments differ, north to south, across the Larsemann Hills. On northern offshore islands, the mafic–felsic orthogneiss is more trondhjemitic, hosts a higher mafic component and is interleaved and infolded with psammite$_2$, associations that are not observed along the southern margin where mafic-felsic orthogneiss is in contact with pelite$_1$. This asymmetry from south to north may represent lateral sedimentary facies variation, but more likely represents structural disturbance.

2.d.1. Metabasite bodies

Discontinuous, concordant lenses and pods of metabasite, consisting of variable amounts of hornblende–plagioclase–biotite ± orthopyroxene ± clinopyroxene, occur within pelite$_3$, semi-pelite, psammite$_1$ and psammite$_3$ units. The primary nature of these metabasite units is problematical. Stüwe, Braun & Peer (1989) suggested that the bulk compositions of two pyroxene–plagioclase 'rafts' were consistent with derivation from meta-igneous precursors, and biotite-bearing, pyroxene-poor varieties have bulk compositions close to felsic orthogneiss, but assumed either a volcanic or intrusive origin. Dirks, Carson & Wilson (1993) assumed an intrusive origin for the metabasite lenses based on (i) the presence of such units within what they assumed to be felsic igneous bodies (their 'granitic gneiss I and II'), and (ii) the correlation of the metabasites with the abundant Proterozoic tholeiitic dykes of the Archaean Vestfold Hills Complex based on a similar geochemical signature. Such geochemical criteria are, however, somewhat inconclusive and ambiguous and the assumption that the metabasite host lithology is of igneous origin is difficult to substantiate. A volcanigenic sedimentary origin for the metabasite units is considered more likely.

The occurrence and abundance of metabasite units is strongly stratigraphically controlled (Fig. 2). Metabasites within the sedimentary pile occur only within mid- to upper units in the described stratigraphy and with increasing abundance (Fig. 3). It is tempting to suggest that this indicates a younging direction, given that basic volcanism is common in the early stages of extensional basin development. If so, the sequence, as described, is inverted.

3. Structural relationships

The structure of the Larsemann Hills is affected by two major high-grade events D_2 and D_3, during which metamorphic conditions reached granulite facies grade. D_2 and D_3 are composite events, each consisting of a number of fold generations and foliation forming events each with identically and uniquely directed fold axes and mineral elongation lineations. D_2 is a major crustal thickening event which is coeval with the metamorphic peak. D_3 is characterized by the development of high-grade shear systems with a normal sense of movement. D_4 consists of a number of discrete high-grade sillimanite-bearing mylonites and D_5 is characterized by the development of planar low-grade brittle features which accommodated minor offsets. The structural nomenclature described here differs significantly from that suggested by Stüwe, Braun & Peer (1989) and any similarity in numbering of deformational schemes is coincidental (Fig. 6). A summary of structural geometries described here is presented in Figure 7.

3.a. D_1 deformation

There is little information concerning the geometry and nature of D_1 deformation. We assign D_1 deformation to post-depositional, early prograde burial and crustal thickening, all of which is obscured by late prograde, peak and subsequent, retrograde metamorphism. Probably the best indication of the

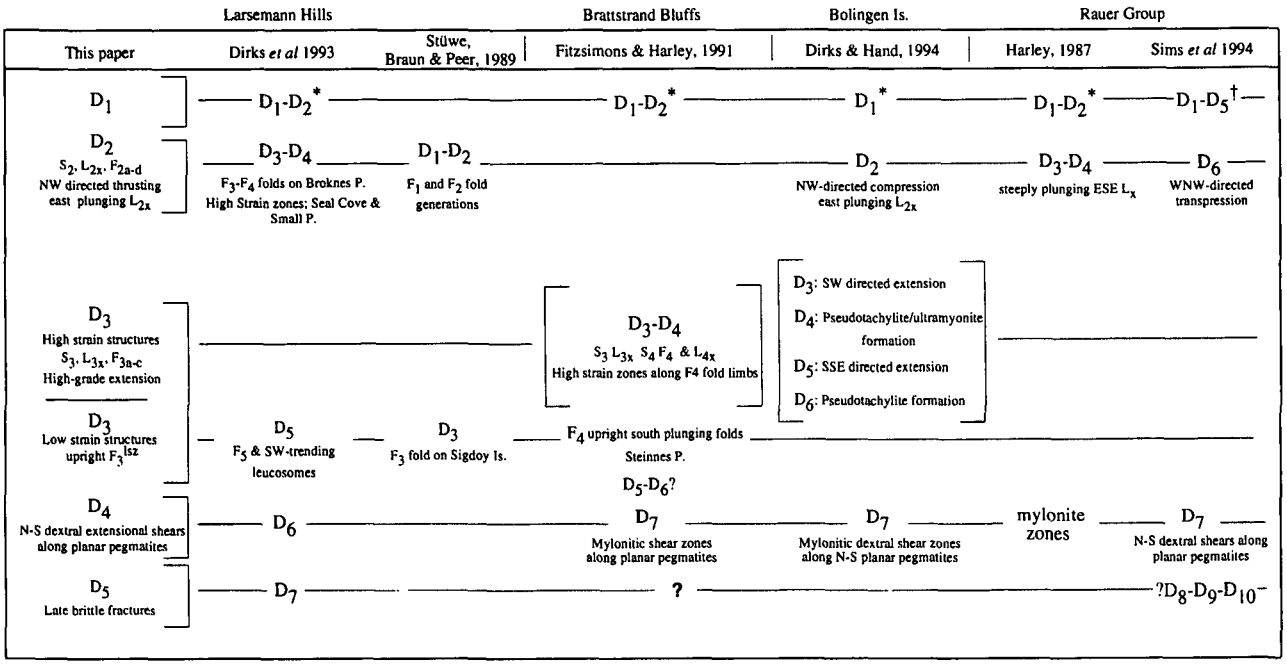

Figure 6. Correlative framework comparing deformation schemes proposed for the southern Prydz Bay region, including the Larsemann Hills, Brattstrand Bluffs, the Bolingen Islands and the Rauer Group. * D_1 and D_2 events listed here represents very early events that are difficult to confidently correlate. † D_1–D_6 of Sims *et al.* (1994) are correlated to structures developed within the Archaean Craton of the Vestfold Hills.

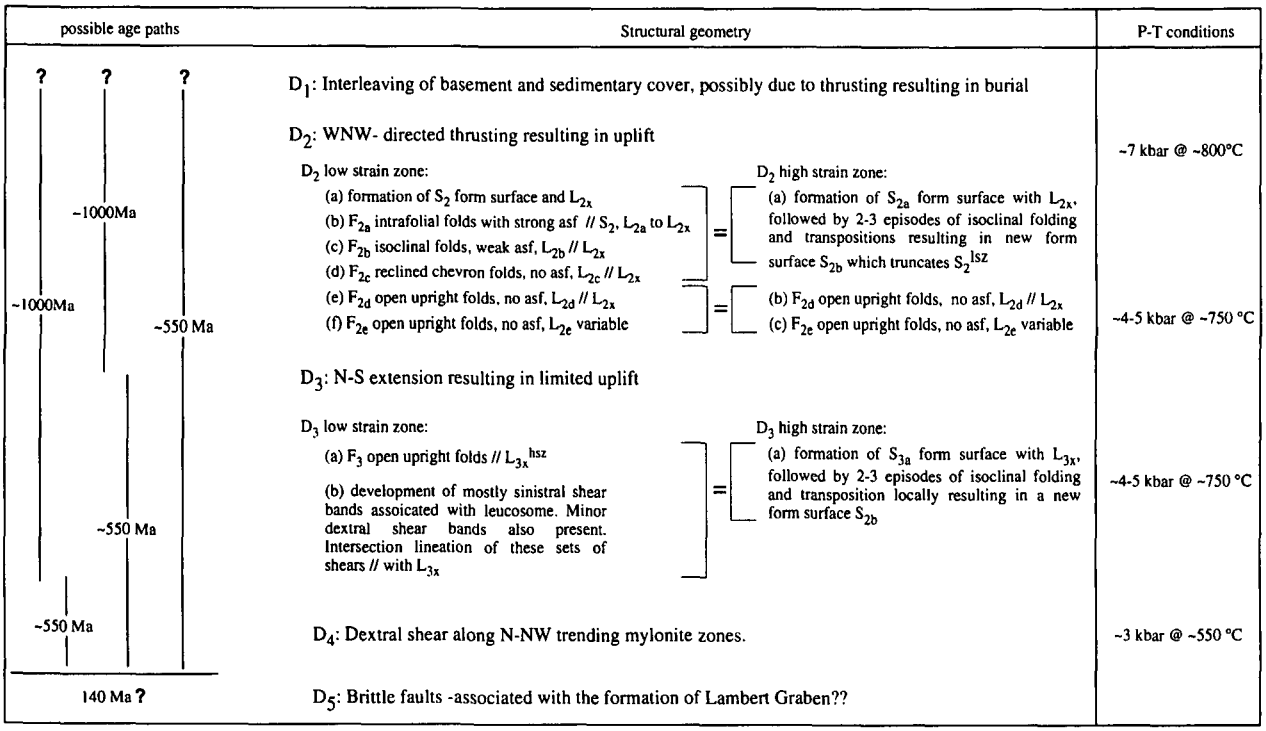

Figure 7. Summary of the structural and geological history of the Larsemann Hills. Possible scenarios for age of deformation events shown on the left. Abbreviations used: asf, axial surface foliation; //, parallel; L_{2a-e}, fold hinge orientation of F_{2a-e}.

nature of D_1 deformation may be derived from the distribution pattern of lithological units across the Larsemann Hills (Fig. 2). Whereas to the south, the assumed lower unit of the stratigraphic sequence is in contact with the basement gneiss, to the north relationships are exactly reversed with basement in contact with some of the assumed highest stratigraphic units. The asymmetrical nature of the cover–basement contact can be well explained by tectonic interleaving and thrust–pile stacking during D_1 thrusting. Evidence for pre-early syn–D_2 event(s) is preserved within peak D_2 garnets from the composite $pelite_2$, $pelite_3$ and

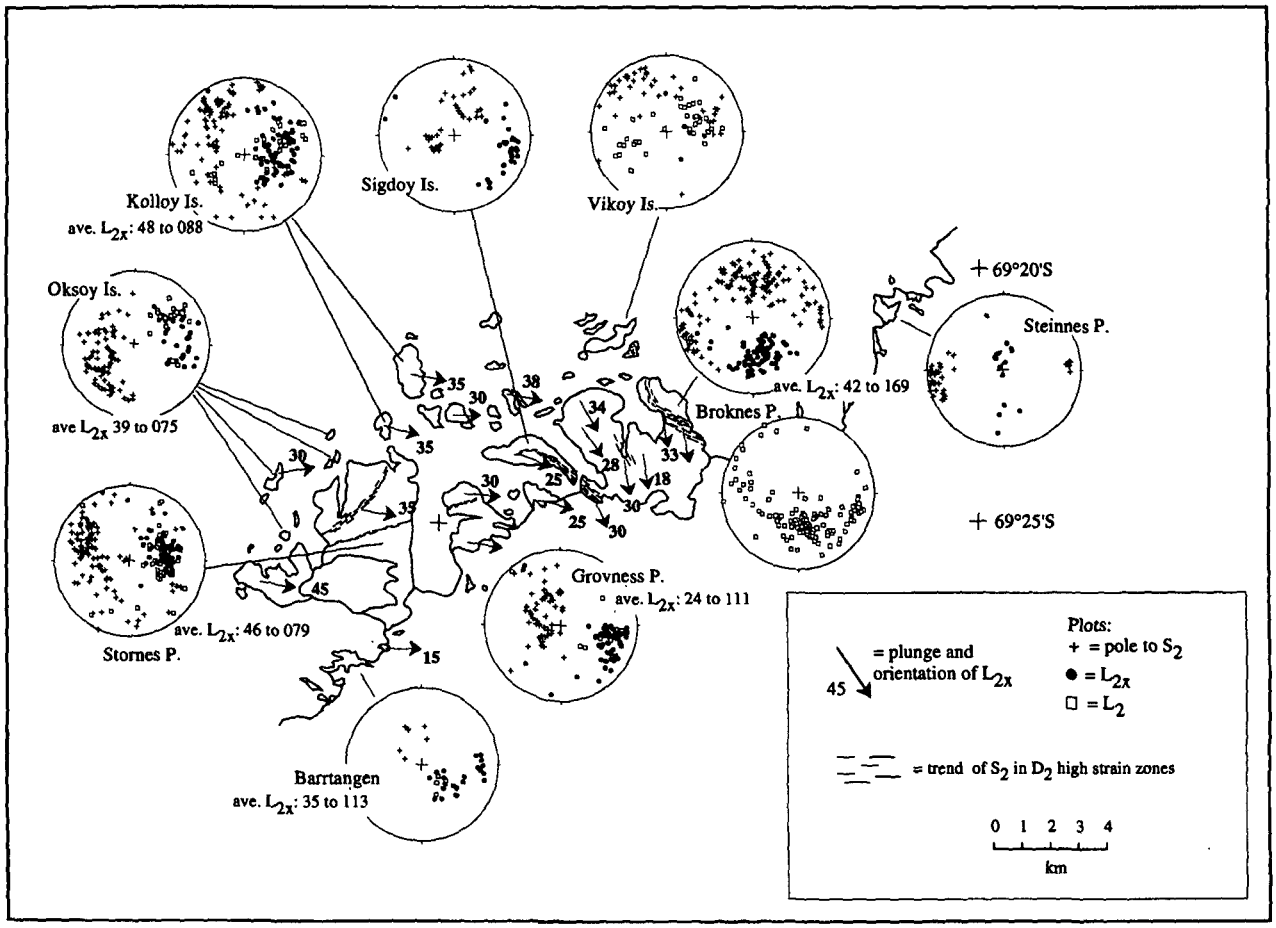

Figure 8. D_2 structural map displaying the regional L_{2x} direction variation across the Larsemann Hills. Note the re-orientation of L_{2x} direction variation across the Larsemann Hills. Note the re-orientation of L_{2x} due to F_3^{isz} folding. The trend of major planar D_2 high-strain zones are also indicated.

semi-pelite, as microscopic, tightly to isoclinally folded, inclusion trails of fibrolitic sillimanite, which are commonly oblique to the pervasive S_2 foliation. Similar micro-textural relationships are described by Fitzsimons & Harley (1991) which are used as evidence of early deformation events ($D_{1\text{-}3(F\&H)}$) from the Brattstrand Bluffs to the northeast. ($D_{x(F\&H)}$ refers to the deformation scheme proposed for the Brattstrand Bluffs by Fitzsimons & Harley, 1991.)

3.b. D_2 thrusting event

The mappable form surface in the majority of the Larsemann Hills formed during D_2. It may consist of a number of truncating foliation generations that are locally complexly folded and has therefore been described for Broknes Peninsula as $D_{2\text{-}4}$ by Dirks, Carson & Wilson (1993). Almost all folds and multiple foliations within D_2 are co-linear, meaning that linear elements including F_2 fold hinges, intersection lineations between various S_2 foliation generations and mineral extension lineations preserved on S_2 surfaces (L_{2x}) are commonly parallel. The average orientation of this lineation direction changes from moderately plunging to east–northeast to east in the western Larsemann Hills to south–southeast on Broknes Peninsula, depending on the relative position of D_2 structures in large-scale D_3 folds (Figs 8, 9).

Regionally, two structural D_2 domains can be distinguished (Fig. 8). These are, (i) zones with a relatively planar, apparently simple gneissic foliation (e.g. Seal Cove and Small Peninsula), which truncate or transpose, (ii) domains with an earlier S_2 form surface that is multiply folded. These domains can be interpreted as high- and low-strain zones respectively. The planar S_2 high-strain zones remain active as ductile shear zones up to the later stages of D_2, whereas the 'low-strain' areas represent domains where S_2 ceased to develop relatively early on during D_2, and further strain was accommodated by progressive co-linear F_2 folding. Based on the co-linearity of linear elements in all D_2 domains, it is assumed they all formed during the one composite D_2 event, associated with a continuous kinematic framework, in this case northwest-directed thrusting (Dirks, Carson & Wilson, 1993, fig. 4e).

3.b.1. F_2 fold sequences

S_2 is folded by at least five progressively developed generations of F_2 folds (F_{2a}–F_{2e}), all of which are not

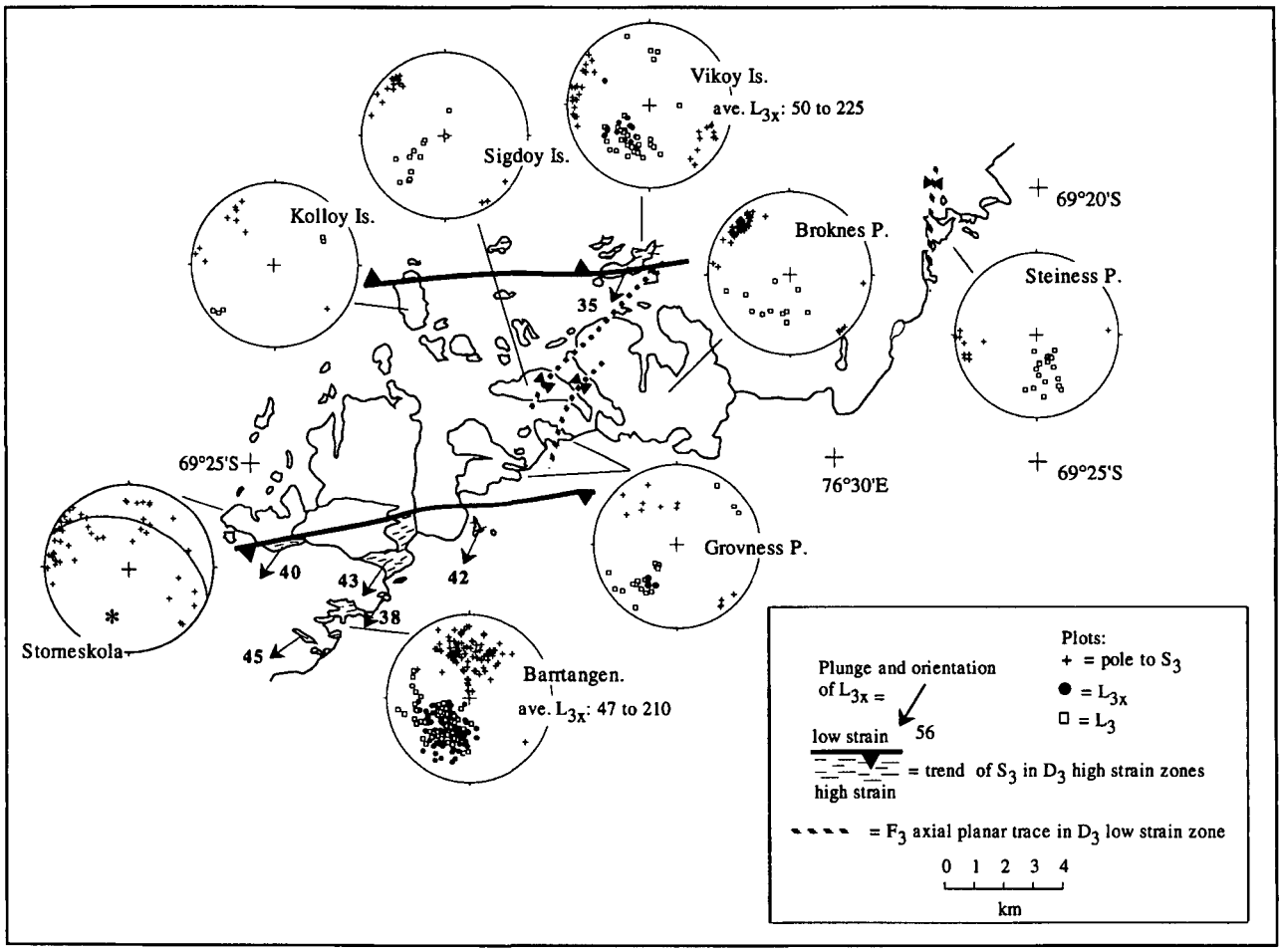

Figure 9. D_3 structural map showing distribution of D_3 high-strain zones and orientation of L_{3x}. Axial traces of major F_3^{lsz} folding on Sigdoy Island and Steinnes Peninsula are shown. Poles to S_3 in D_3 low-strain domains combine of F_3^{lsz} fold axial surfaces and shear band orientations. The stereo plot for the Storneskola region contains poles to S_3^{lsz} shear bands. Note that the intersection lineation of these planes are co-linear to the regional L_{3x} lineation, indicated by the asterisk.

necessarily present in any one location. F_{2a} folds have only been observed on outcrop-scale, and are rare isoclinal intrafolial folds with a moderate to strongly developed axial planar foliation (S_{2a}) defined by biotite, sillimanite and compositional layering (Fig. 10a). S_{2a} is only identifiable within the fold closure, but is otherwise indistinguishable from the S_2 foliation it folds. The hinge region commonly has a characteristic 'feathered' or flame-like appearance as the folded lithological contact is irregular (Fig. 10a). F_{2b} tight to isoclinal folds are similar to F_{2a} folds, and are characterized by a weak axial surface foliation (S_{2b} generally defined by biotite and/or sillimanite, and a more regular fold surface. F_{2c} folds are macroscopic ($\sim$ 200–400 m amplitude), open to tight, folds with inclined to recumbent axial surfaces and angular hinge regions giving them a chevron fold appearance. Axial surface foliations are absent or weak and only developed in biotite-rich units. Good examples of these folds can be seen on eastern Stornes Peninsula, Eliza Kate and Breadloaf islands (Fig. 2). F_{2a-c} folds can only be found in the low-strain D_2 domains. They may have been present in the high-strain zones as well, but in that case all evidence is completely obliterated due to intense transposition. In contrast the common F_{2d} folds are present in all D_2 domains. They vary in scale from 1–5 mm crenulations of biotite, to 5 m wide, upright to slightly reclined, open to closed cylindrical folds that contain no axial planar foliation. In outcrop F_{2a-d} fold generations are co-linear with the ambient mineral extension direction (L_{2x}) present on S_2 (Fig. 10b), although variations in absolute orientation occur due to late D_3 folding (Fig. 8). A final set of F_{2e} folds are open to tight upright folds that differ from previous generations in that they can locally fold L_{2x}.

Within the relatively planar high-strain zones, a number of fold types may be present. In general one or more generations of tightly to isoclinally folded, highly disharmonic, parallel folds may be distinguished, some of which preserve sheath fold geometries that are not everywhere absolutely co-linear with the ambient mineral extension lineation. These folds are subsequently overprinted by F_{2d-e} type folds.

Although S_2, especially in the high-strain zones, may be equated with a non-coaxial flow foliation,

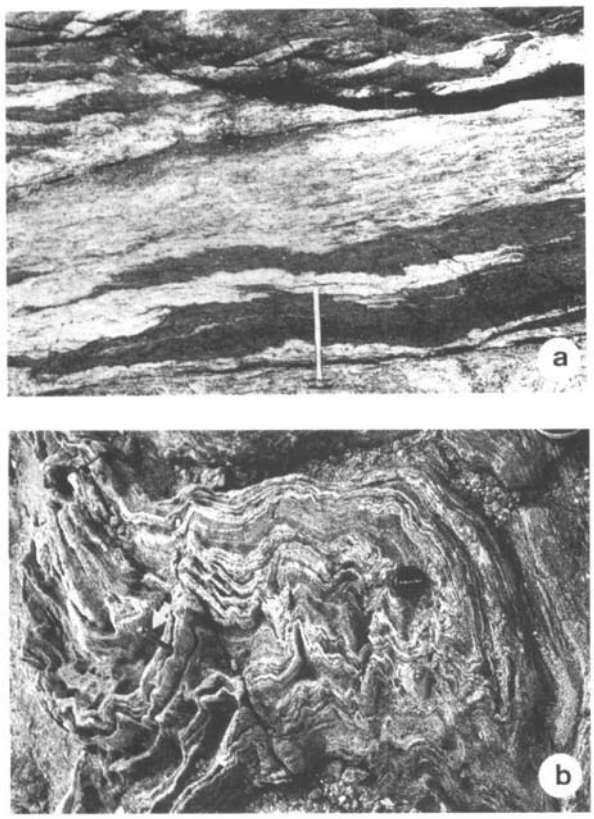

Figure 10. (a) Typical F_{2a} fold with 'flamelike' geometry and characteristic strong axial surface fabric, Stornes Peninsula. Hammer handle ~ 0.75 m. (b) Interference pattern of co-linear F_{2b-d} folds viewed in a plane normal to the lineation, Broknes Peninsula. Pencil (arrowed) indicates direction of L_{2x} and fold hinge.

kinematic indicators in S_2 are infrequent (Fig. 11). They are restricted to uncommon mesoscopic fold asymmetries for folds that are not co-linear with L_{2x} (fig. 4e of Dirks, Carson & Wilson, 1993), leucosome-filled shear bands and rotated boudins, all of which are consistent with west- to northwest-directed thrusting if the current orientation of the D_2 high-strain zones is taken as a reference frame (Dirks, Carson & Wilson, 1993).

3.c. D_3 extension event

A second major composite event, D_3, overprints and locally transposes D_2 structures. These are completely replaced by a new gneissic layering, S_3, on the north and south sides of the Larsemann Hills (Fig. 9). Therefore, the larger part of the Larsemann Hills represents a window of low D_3 strain in which D_2 deformation is largely preserved.

D_3 structures can be categorized in the same manner as D_2 structures with (a) D_3 high-strain zones where a number of truncating foliations, with the same mineral elongation lineation direction, are paralleled by various generations of F_3 fold hinges, and (b) D_3 low-strain domains where S_2 constitutes the form surface and D_3 effects are limited to later folds, shear bands, migmatite development and partial metamorphic re-equilibration. The average L_{3x} orientation plunges 47° to 210° with all generations of F_3 fold axes sub-parallel to this orientation in both high- and low-strain areas (Fig. 9). In regions transitional from S_2- to S_3-dominated domains, two lineations may be preserved on foliation surfaces, that is, in semi-pelite on southern Stornes Peninsula, L_{3x} sillimanite–spinel lineations overprint an earlier east-plunging L_{2x} lineation defined by sillimanite and aligned 'trails' of large (5–20 mm diameter), subhedral garnet.

3.c.1. F_3 fold generations and low-strain structures

Fold sequences in D_3 differ from D_3 high-strain zones to low-strain D_3 domains. In D_3 high-strain zones the sequence of fold geometries are similar to those described for D_2 high-strain zones. Early intrafolial folds (F_{3a}) are refolded by up to two generations of tight to isoclinal folds (F_{3b-c}) with generally weak to no axial planar foliations and a late generation of upright, closed to open F_{3d} folds.

F_3 folds in low-strain D_3 domains (F_3^{lsz}) are generally upright open to isoclinal folds with axial surfaces that dip around 80° towards 100–130° with fold hinges paralleling the regional L_{3x} recorded from D_3 high-strain zones. Fold amplitudes vary from several centimetres to several kilometres and two major F_3^{lsz} folds can be recognized on Sigdoy Island and Steinnes Peninsula (e.g. upright south plunging $F_{4(F\&H)}$ structure (fig. 3a of Fitzsimons & Harley, 1991). Large-scale F_3^{lsz} folding is responsible for major re-orientation of D_2 structural elements (Figs 8, 9). Along the axial surface trace of the major open F_3^{lsz} fold that runs through Sigdoy Island, numerous small-scale parasitic folds are present (Fig. 12a). On Foxtrott Oskar Island and Vikoy Island interference of these small scale folds with upright F_{2d} folds produces type 1 fold interference geometries. The F_3^{lsz} structure on Sigdoy Island is relatively open compared with the F_3^{lsz} tight to isoclinal major and parasitic fold structures on Steinnes Peninsula (Fig. 3), suggesting intensification of D_3 strain towards the northeast. Similarly, Fitzsimons & Harley (1991) report $D_{4(F\&H)}$ (= D_3 this paper) strain intensification northeast from Steinnes Peninsula to the Brattstrand Bluffs with 'increasing structural depth' (e.g. figs 3b, 7 and 8 of Fitzsimons & Harley, 1991; fig. 2 of Fitzsimons & Harley, 1992). An alternative description, however, is a progressive transition from a D_3^{lsz} which preserves upright F_3^{lsz} structures folding an S_2 foliation, intensifying to the northeast into D_3 high-strain zone, dominated by S_3 foliation (= $S_{4(F\&H)}$), transposing D_3^{lsz} structures.

Additional D_3 structures that are present in low-strain domains are sets of asymmetrical crenulation bands or cleavage boudins (Platt & Vissers, 1980) that form discrete discontinuous ductile shear bands,

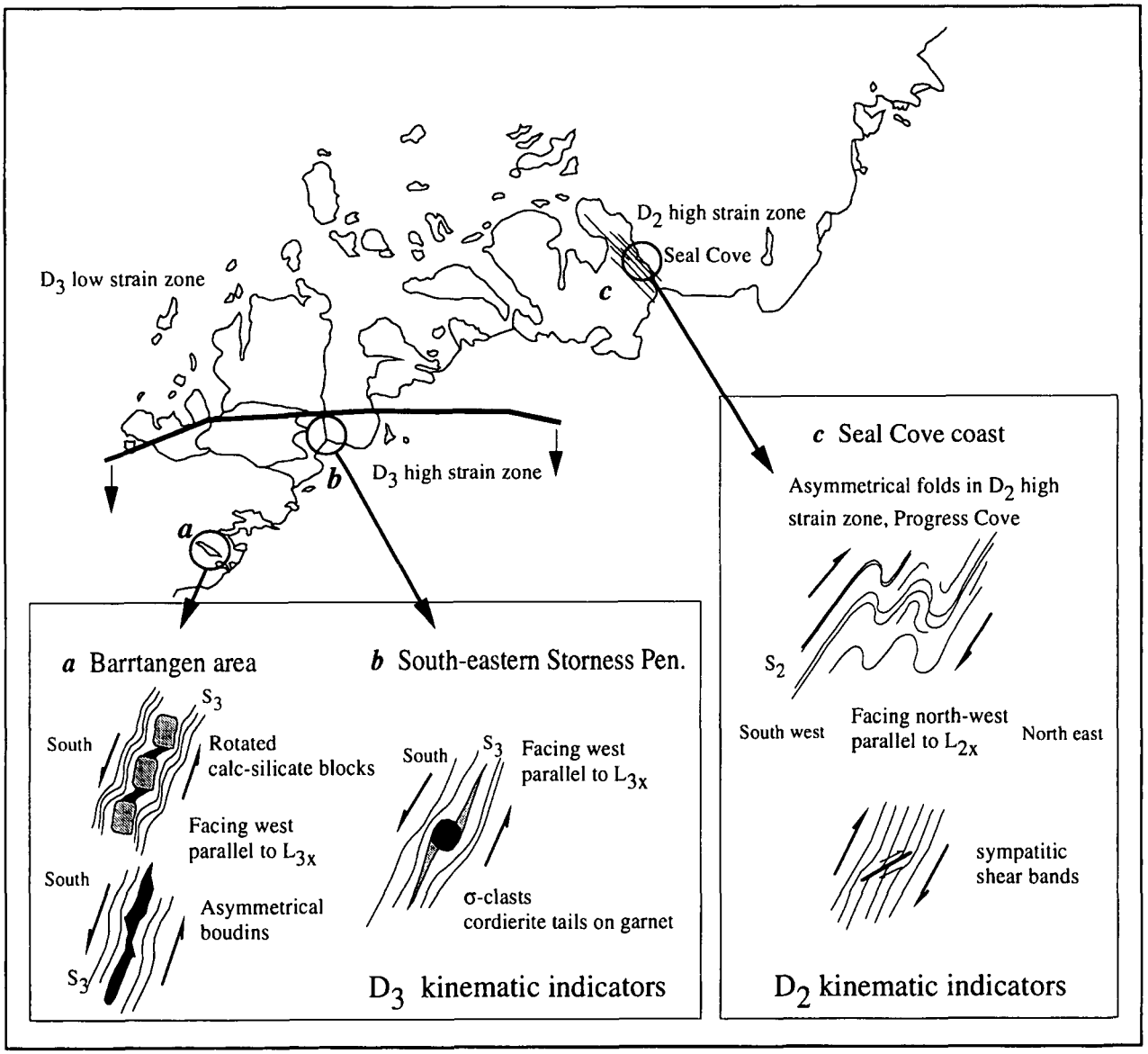

Figure 11. Map showing the location and nature of various kinematic indicators for both D_2 and D_3 domains.

commonly with co-planar leucosome development (Fig. 12b). Within exposures west of the F_3^{lsz} fold trace through Sigdoy Island such shear bands are limited to one set which is upright to steeply dipping (toward ~ 130°) with generally an apparent sinistral movement sense in plan view. To the east of this fold trace (Broknes Peninsula), leucosome-bearing sinistral shear bands occur as overprinting sets displaying a progressive clockwise rotation from old to young (= $S_{5a,b,c}$, Dirks, Carson & Wilson, 1993). This suggests that the west limb of the major F_3^{lsz} fold was stable in the D_3 stress field whilst the east limb rotated. This also indicates that the east-plunging direction of L_{2x} is likely to be closest to its original orientation. The upright D_3 shear bands and associated leucosomes are also developed in the axial surfaces of mesoscopic, parasitic F_3^{lsz} folds on Foxtrott Oskar, Fold, and Sigody islands, where they are associated with offsets of up to 0.5 m in the hinge region (Fig. 12b). Within extreme southwest exposures (e.g. Storneskola), D_3 sinistral shear bands form conjugate sets with a set dipping moderately toward 200° and with a dextral sense in plane view. The transport vector, where recorded, is sub-parallel to L_{3x} in D_3^{hsz} domains which also parallels the intersection lineation of the conjugate D_3^{lsz} shear bands (Fig. 9).

Kinematic indicators in S_3 high-strain domains consistently preserve a south-down normal movement sense with a minor dextral component (Fig. 11). These indicators include shear bands, back-rotated calc-silicate boudin blocks (Fig. 12c) and asymmetrical metabasite boudins in mafic–felsic orthogneiss (Barrtangen), and rare σ-blasts defined by cordierite mantles on garnet (Fig. 12d, southern Stornes Peninsula). The locations of major D_3 kinematic indicators are shown on Figure 9.

The composite D_3 event in the Larsemann Hills equates with $D_{3\text{-}4(F\&H)}$ events reported from the

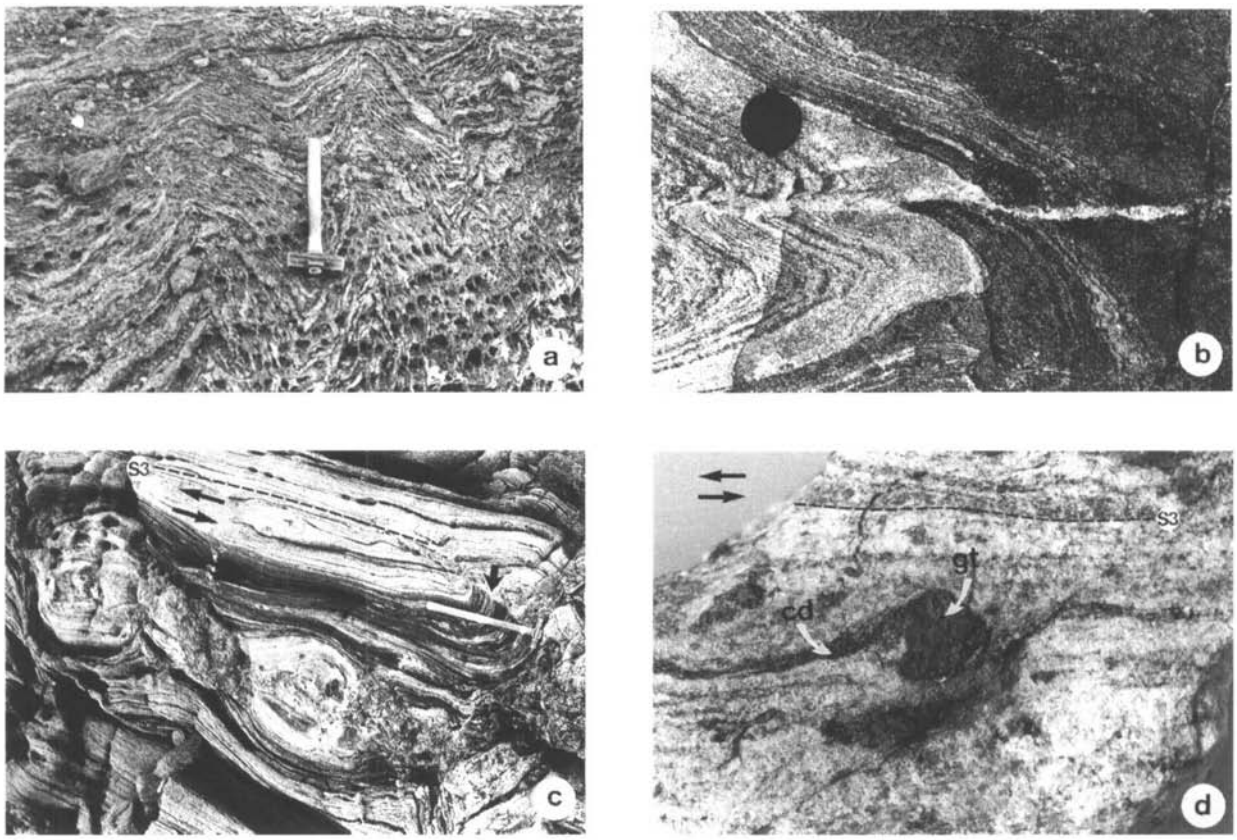

Figure 12. (a) Mesoscopic upright F_3^{lsz} folds in the hinge region of the major F_3^{lsz} structure on Sigdoy Island. (b) Syn-D_3 shear bands containing leucosome, developed along an F_3^{lsz} fold, Fold Island (c) a train of back-rotated calc-silicate blocks, embedded in a matrix of composite orthogneiss, Barrtangen. View facing west, base of the photograph to right. Foliation present S_3, L_{3x} parallel with photograph. Arrow near hammer shows small asymmetrical, south-down folds. Hammer handle ~ 0.75 m. (d) σ-blast of garnet (gt) with recrystallized tails of cordierite (cd) and spinel, which developed within the D_3 high-strain zone on southern Storness Peninsula. View facing west, foliation present S_3, L_{3x} parallel with photograph. Field of view ~ 75 × 100 mm.

Brattstrand Bluffs coastline to the northeast. Both a tightly folded foliation, $S_{3(F\&H)}$, and a flat-lying shear foliation, $S_{4(F\&H)}$, preserves a predominantly south-plunging lineation ($L_{3(F\&H)}$ and $L_{4(F\&H)}$), similar to the composite S_3 foliation and L_{3x} lineation presented here for the Larsemann Hills. $F_{4(F\&H)}$ fold axes parallel this $L_{4(F\&H)}$ similar to the co-linear nature of multiple F_3 fold generations developed in the southern Larsemann Hills.

3.d. D_4 deformation

D_4 deformation is confined to the development of up to 20 cm wide, upright amphibolite-grade mylonite zones that formed along planar north–south-trending garnet–sillimanite–spinel-bearing pegmatites (D_6, Dirks, Carson & Wilson, 1993; Fig. 13a). These mylonites are best developed on the western Broknes Peninsula and Sigdoy Island, and are relatively uncommon elsewhere. The movement sense is typically dextral, east-down (fig. 6 of Dirks, Carson & Wilson, 1993) along a 20–30°S pitching sillimanite lineation, and offsets are generally less than 20 m. Within pegmatites, S_4 is defined by sillimanite and quartz ribbons, whilst garnet and Zn-spinel (~ 6 wt % ZnO) are stable. K-feldspar porphyroclasts are semi-plastically deformed and develop asymmetrical tails that are stretched along S_4. Planar north–south orientated fractures that contain garnet, cordierite, quartz, magnetite and randomly orientated biotite, occur both adjacent to, and distal from, D_4 mylonite zones, and are considered to have formed syn-D_4. No offset is associated with these fractures (Fig. 13b). The stability of garnet, sillimanite, Zn-spinel and K-feldspar in D_4 mylonites, and garnet, cordierite and biotite in planar fractures suggests at least amphibolite grade conditions during D_4. Similar planar pegmatites with sheared margins occur throughout the Prydz Bay region (see, e.g. Harley, 1987; Fitzsimons & Harley, 1991; Figure 6).

3.e. D_5 deformation

D_5 deformation is restricted to uncommon planar, sub-vertical brittle faults with variably developed sub-horizontal slickenlines and abundant epidote. These have been described as D_7 by Dirks, Carson & Wilson (1993).

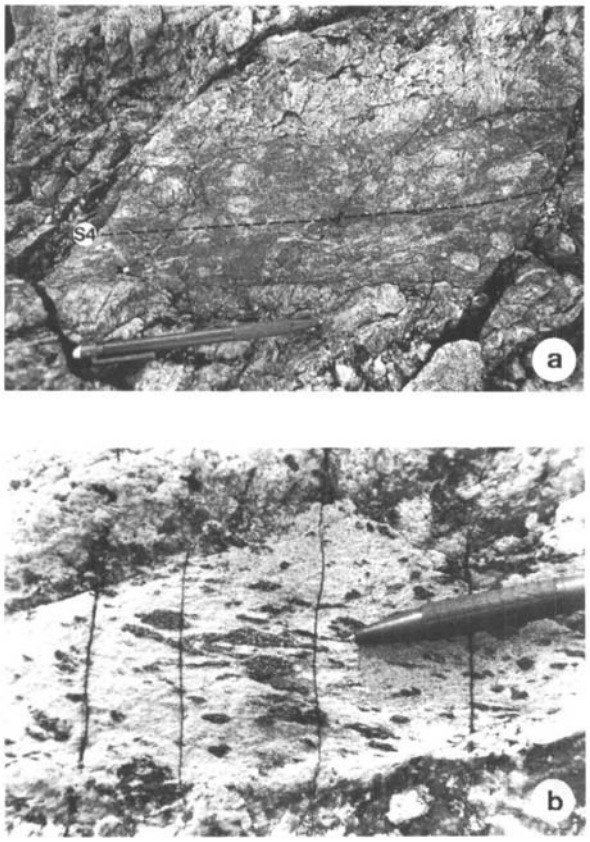

Figure 13. (a) D_4 mylonite zone developed along margin of N–NW trending planar pegmatites, Broknes Peninsula. (b) Biotite-cordierite fractures developed parallel to D_4 mylonites. Southern Stornes Peninsula.

4. Structural–metamorphic relationships

This section describes metamorphic textures in reference to the structural–kinematic framework and briefly outlines preliminary pressure–temperature estimates. The textures observed within metapelitic units are consistent with many of the textural features observed in metapelitic sequences of the Brattstrand Bluffs (Fitzsimons & Harley, 1991, 1992).

4.a. Domains with S_2 as dominant foliation

S_2 assemblages preserved within $pelite_1$, composite $pelite_2$ and $pelite_3$ contain variable amounts of garnet, cordierite, quartz, plagioclase, K-feldspar, spinel, sillimanite and biotite. Two textural varieties of garnet are commonly present. $Garnet_1$ is strongly corroded and generally elongate in S_2 and L_{2x}, and characterized by abundant inclusions of tightly folded fibrolitic sillimanite and $biotite_1$. Inclusion-free moats separate sillimanite and $biotite_1$ within $garnet_1$, suggesting destabilization of early biotite–sillimanite to form $garnet_1$ (Grant, 1985; cf. Brattstrand Buffs, Fitzsimons & Harley, 1991, 1992) via the prograde reaction:

$$\text{biotite} + \text{sillimanite} + \text{quartz} = \text{garnet}_1 + \text{K-feldspar} + \text{melt}, \quad (1)$$

early during D_2. $Garnet_1$ and early foliation forming, $spinel_1$ are separated by cordierite moats which may form coarse-grained overgrowths aligned in S_2 or delicate symplectic intergrowths with plagioclase, quartz and $spinel_2$. Possible retrograde reactions include:

$$\text{garnet}_1 + \text{spinel}_1 = \text{cordierite} + \text{plagioclase} \quad (2)$$

and

$$\text{garnet}_1 + \text{sillimanite} = \text{cordierite} + \text{quartz} + \text{spinel}_2. \quad (3)$$

The coarse-grained cordierite overgrowths consist of large (several mm) grains with relatively straight grain boundaries suggesting textural re-equilibration after formation of the coronas in response to syn-D_2 decompression. This type of texture is very common in the semi-pelite. In contrast the delicate symplectic intergrowths involving cordierite are in textural disequilibrium and must have formed relatively late. Although many of these are also aligned in S_2or L_{2x}, this may have resulted from replacement of D_2 phases rather than syn-D_2 growth, and the origin of these symplectites including $spinel_2$ is probably syn-D_3. This is suggested by the common occurrence of such symplectites in D_3 high-strain zones.

Although inclusion trails in $garnet_1$ suggest that sillimanite and biotite were not stable during peak-D_2 in quartz-bearing pelites (see above), matrix sillimanite and biotite in combination with a second generation garnet are very common in these assemblages. $Garnet_2$ occurs as inclusion-free subhedral grains, which may mantle $garnet_1$. The renewed stability of biotite generally and of the assemblage garnet, sillimanite, biotite, quartz in pelites probably occurred during D_3 as this assemblage is common in D_3 high-strain zones. It suggests hydration and/or cooling of the terrain which is consistent with the growth of various borosilicates at the onset of D_3, due to an influx of a fluid (possibly boron-enriched, Carson, Hand & Dirks, 1995), which is consistent with the stabilization of biotite in S_4 zones in the Brattstrand Bluffs (Fitzsimons & Harley, 1991, 1992). The presence of narrow coronas of cordierite and rarely biotite on $spinel_{1+2}$ in the presence of quartz probably represents late syn- to post-D_3 cooling (see, e.g. Fitzsimons & Harley, 1992). This is also consistent with thin coronas of garnet on hornblende and orthopyroxene in metabasite lenses on Steinnes Peninsula.

Trails of garnet, orthopyroxene, plagioclase defining S_2 and L_{2x} are common within the Grovness enderbite, and corroded grains of garnet are in contact with orthopyroxene. This is a feature that is also common in many of the metabasite layers that occur within part of the stratigraphy. Preliminary geothermobarometry relevant to orthopyroxene–garnet–plagioclase–quartz assemblages (Harley & Green, 1982; Newton & Perkins, 1982; Harley, 1984*a*, *b*; Sen

& Bhattacharya, 1984) based on core compositions of coexisting orthopyroxene–garnet pairs yield peak conditions of ~ 7 kbar and ~ 780 °C. These peak *P–T* conditions compare favourably with previously reported peak conditions reported in the nearby Bolingens Island (e.g. 6 kbar, ~ 760 °C, Motoyoshi, Thost & Hensen, 1991) and the Reinbolt Hills (7 kbar, ~ 800 °C, Nichols & Berry, 1991, fig. 1) to the south and from the Brattstrand Bluffs to the north (6 kbar, ~ 850 °C, Fitzsimons & Harley, 1991, 1992).

4.b. Domains with S_3 as dominant foliation

Relevant textures from metabasites with D_3 domains include the destabilization of garnet generating orthopyroxene and plagioclase symplectites which are enveloped by a biotite S_3 foliation. On Barrtangen such coronas contain fine platelets of symplectic biotite that are aligned parallel with the external S_3 foliation. Within basement composite orthogneiss on Fold Island, hornblende, plagioclase, orthopyroxene-bearing metabasite preserves orthopyroxene, plagioclase, biotite ± clinopyroxene symplectites that are strongly elongate in the regional L_{3x} direction. These textures may represent destabilization of garnet, now consumed, via the retrograde reactions:

$$\text{garnet} + \text{quartz} = \text{orthopyroxene} + \text{plagioclase} \quad (4)$$

and

$$\text{garnet} + \text{quartz} + \text{hornblende} = \text{orthopyroxene} + \text{plagioclase} + H_2O, \quad (5)$$

indicative of decompression (see, e.g. Harley, 1988; Nichols & Berry, 1991; Clarke & Powell, 1991). On Kolloy and northwest Vikoy islands, coarse-grained biotite selvedges commonly occur at the contact of felsic and mafic sub-units of the basement orthogneiss. The contact is folded by open to tight upright F_{3d} folds, and biotite in the selvedge develops a well-developed preferred orientation parallel to the axial plane of the F_{3d} folds. Within the biotite selvedge, coarse-grained garnet develops a plagioclase corona that overprints the biotite S_{3d} foliation, indicating post-S_{3d} garnet breakdown.

Within semi-pelite from the D_3 high-strain zone on southern Storness Peninsula, $garnet_1$ is locally overgrown by a mantle of inclusion-free $garnet_2$ and wrapped by sillimanite aligned in L_{3x}. Garnet and sillimanite are subsequently consumed by cordierite that is elongated in tails along L_{3x}. Within nearby pelite, trails of $garnet_1$ aligned in L_{2x} are wrapped by sillimanite aligned in L_{3x}. Garnet is subsequently consumed by L_{3x}-parallel, delicate cordierite–spinel symplectites, via reaction (3).

Preliminary *P–T* results using the quantitative average *P–T* approach outlined by Powell & Holland (1994) give very similar results for D_2 and D_3 domains using the various matrix and corona assemblages. Mineral zoning in garnet, cordierite or spinel is minimal, as are most compositional variations in texturally different generations of these minerals (Carson, unpub. data). $Pelite_1$, composite $pelite_2$, $pelite_3$ and metabasite lenses from D_2 and D_3 domains record pressures around 4 to 5 kbar, over a range of temperatures between 650–800 °C.

P–T estimates on the amphibolite-grade assemblages in D_4 mylonites using garnet–biotite geothermometry (Ganguly & Saxena, 1984; Bhattacharya *et al.* 1992) and average pressure–temperature calculations of Powell & Holland (1994) result in pressures of ~ 3.0 kbar at ~ 550–650 °C.

5. Structural–metamorphic correlations

The similarity of pervasive structural features, orientations and kinematics along the Prdyz Bay coast, enables apparently simple correlations of structural and metamorphic events. These correlations are limited to the 'Neoproterozoic' terrains and cannot be made to the Archaean Vestfold Hills Block.

In the Bolingen Islands immediately southwest of the Larsemann Hills (Fig. 1), Dirks & Hand (1995) describe dominantly east–west-trending, south-dipping foliations that contain an early, east-plunging lineation related to thrusting in the south Boligen Islands and a later south-plunging lineation related to normal movements in the north Bolingen Islands. This latter zone is the direct westward extension of the D_3 high-strain zone in Barrtangen. Thus, D_2 and D_3 domains similar to those in the Larsemann Hills are readily apparent in the Bolingen Islands, which are also truncated by later pegmatites paralleled by amphibolite grade shear zones. Thost, Hensen & Motoyoshi (1991) report peak conditions of 10 kbar and 980 °C from basement gneiss in the southwest Bolingen Islands, using garnets which Dirks & Hand (1995) describe as being aligned in L_{2x}. Thost, Motoyoshi & Hensen (1988) and Thost, Hensen & Motoyoshi (1992) also report a second metamorphic overprint (syn-D_3 ??) of ~ 6 kbar and ~ 775 °C from the same area, which is comparable with *P–T* results of ~ 6 kbar and ~ 760 °C obtained from calc-silicate units elsewhere in the Bolingen Islands (Motoyoshi, Thost & Hensen, 1991).

In the Brattstrand Bluffs some 30–35 km northeast of the Larsemann Hills (Fig. 1) a similar metasedimentary sequence is described by Fitzsimons & Harley (1991, 1992). They identified a shallowly south-dipping planar foliation ($S_{4(F\&H)}$), truncating a tight to isoclinally folded $S_{3(F\&H)}$ foliation which itself contains colinear intrafolial folds. Both foliations, S_3 and $S_{4(F\&H)}$, preserve a south-plunging mineral extension lineation. These structures record a normal sense of movement (Fitzsimons & Harley, 1991, 1992; Dirks & Carson, unpub. data) and can be correlated with the progressively folded and truncated foliations in D_3 normal shear domains from the Larsemann Hills,

while earlier assemblages in low-strain zones and inclusions (called D_1 and D_2 by Fitzsimons & Harley, 1991) may represent D_2 features. Coarse-grained garnets, rapped in the south-plunging lineation (L_{3x} and $L_{3,4(F\&H)}$) can contain inclusions of prismatic sillimanite (texturally distinct from isoclinally folded fibrolitic sillimanite trails) which are aligned sub-parallel to the regional L_{2x} direction and may represent the preservation of D_2 features in the Brattstrand Bluffs.

Fitzsimons & Harley (1991, 1992) previously report peak *P–T* estimates of 6 kbar and 850 °C followed by decompression and cooling to 3–4 kbar and 770 °C, conditions that are near identical to those now identified in the Larsemann Hills. Rocks in the Brattstrand Bluffs are also truncated by a late set of north–south pegmatites with sheared margins ($D_{7(F\&H)}$).

The Rauer Group (Fig. 1) is dominated by a series of progressively overprinting co-linear folds and foliations recording a very constant fold axes and mineral lineation plunging moderately to the southeast (see, e.g. Harley, 1987; Sims *et al.* 1994), and is associated with thrust kinematics (Dirks *et al.* 1993; Sims *et al.* 1994). Most of this deformation may be equivalent to the composite D_2 event recorded from the Larsemann Hills. It is associated with decompression of ~ 2–4 kbar from peak conditions of 7–9 kbar at temperatures in excess of 850 °C (Harley, 1988; Harley & Fitzsimons, 1991), dated at 1000–1050 Ma (zircon U–Pb, Kinny, Black & Sheraton, 1993). Although a new zircon population with an age of ~ 500 Ma is common in a large variety of lithologies in the Rauer Group (Kinney, Black & Sheraton, 1993), the only events definitely linked to the Pan-African are north–south trending pegmatite dykes (500 ± 12 Ma, Kinny, Black & Sheraton, 1993), with amphibolite-grade shear zones at their margins.

The Landing Bluff granitoid units (Fig. 1) contain mafic layers and biotite-rich schlieren that preserve one generation of open upright folds, with fold hinges that are co-linear with the regional D_3 lineation, similar to that recorded from the Larsemann Hills, Brattstrand Bluffs (Fitzsimons & Harley, 1991) and the Bolingen Islands (Dirks & Hand, 1994). These granitoid units are widely accepted as Pan-African post-orogenic instrusives by most workers (e.g. Stüwe, Braun & Peer, 1989; Sheraton, Black & McCulloch, 1984; Fitzsimons & Harley, 1991), for which a 493 ± 17 Ma Rb–Sr age (whole rock) has been obtained (Tingey, 1981). Given that the granitoids preserve one generation of F_3 folding, however, suggests that these granitoid bodies intruded late syn-D_3. Additionally, moderately west-dipping planar coarse-grained pegmatites cross-cut these granitoids, again similar to those reported elsewhere in Prydz Bay.

Using the orientation of the dominant linear features and kinematic indicators in high-grade foliations, it is simple to correlate D_2, D_3 and D_4 events along the length of Prydz Bay. Figure 6 summarizes the structural and geochronological correlations in southeastern Prydz Bay.

6. Timing of the structural events

Most of the pervasive deformational and metamorphic features of eastern Prydz Bay outcrops, south of the Archaean craton of the Vestfold Hills, have been previously assumed to have evolved during a tectonic event that occurred ~ 1000 Ma ago (see, e.g. Fitzsimons & Harley, 1991, 1992; Harley *et al.* 1992; Harley & Fitzsimons, 1991; Thost, Hensen & Motoyoshi, 1991; Sheraton, Black & McCulloch, 1984; Stüwe, Braun & Peer, 1989; Stüwe & Powell, 1989*a*). While syn-deformational orthogneiss units from the Rauer Group strongly indicate a significant ~ 1000 Ma tectonothermal event in that area (Kinny, Black & Sheraton, 1993), the effects of the Pan-African orogeny in the Prydz Bay area are previously thought to be limited to low-grade discrete shear zones (e.g. Kinny, Black & Sheraton, 1993; Harley, 1987; Fitzsimons & Harley, 1991) and various post-orogenic intrusive bodies (e.g. Tingey, 1981). Recent geochronology in the Larsemann Hills, however, suggests a major metamorphic imprint of Pan-African age (~ 550 Ma).

Sm–Nd isochron ages from mafic gneiss and Zhong Shan Gneiss near Zhong Shan station (Fig. 2) yield Pan-African ages (whole rock–orthopyroxene–hornblende–plagioclase, 540 ± 75 Ma; whole rock–garnet–K-feldspar, 497 ± 7 Ma, respectively, Zhao *et al.* 1993). Step-wise evaporation $^{206}Pb/^{207}Pb$ techniques applied to zircon separates (Kober, 1986, 1987) from the Progress granite yield core ages of 547 ± 9 Ma which is interpreted to approximate the crystallization age of the granite (Zhao *et al.* 1992). The Progress granite on Mirror Peninsula truncates all F_2 fold generations and contains a variable though generally weak biotite foliation that is generally concordant with the pervasive S_2 foliation in the host gneiss. The granitic foliation can be discordant by up to 30° with the external S_2 gneissic foliation. The granite is elongated in the D_2 high-strain zone, however, it is not certain that this is a D_2 deformational effect. At Barrtangen, however, the Progress granite is isoclinally folded and strongly transposed with the pervasive S_3 high-strain zone foliation and K-feldspar and biotite are aligned in L_{3x} (Fig. 14), whilst on Steinnes Peninsula, this unit occurs in the core of the major F_3^{lsz} structure and is folded by that structure. These observations suggest a relative intrusive age for the Progress granite to syn-S_2–pre-S_3.

When considering the above ages for these intrusive units and their relevance for tectonic interpretations, it is important to consider whether they represent real crystallization ages. Zhao *et al.* (1992) argue that the

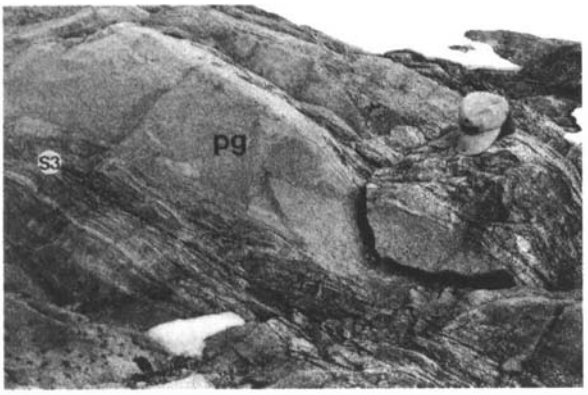

Figure 14. Tightly folded and sheared contact between progress granite (labelled 'pg') and pelite$_1$ within the D_3 high-strain zone on Barrtangen. Hat ~ 250 mm wide.

$^{206}Pb/^{207}Pb$ zircon ages obtained from the Progress granite represent a primary crystallization age because the reported zircon populations are homogeneous and display clear age plateaus that suggest no serious radiogenic Pb loss. An alternative interpretation is that the $^{206}Pb/^{207}Pb$ system suffered very serious radiogenic Pb loss, resulting in effective homogenization of the zircon's radiogenic Pb profile during a Pan-African thermal event. The ages may, therefore, simply represent Pan-African reset ages. Sm–Nd ages obtained from various lithologies (Zhao *et al.* 1993), may also represent Pan-African reset ages, given that recent studies on closure temperatures for Sm–Nd systematics can be as low as 600 °C (see, e.g. Mezger, Essene & Halliday, 1992). A number geochronological–structural scenarios are therefore possible (Fig. 7).

Assuming that the $^{206}Pb/^{207}Pb$ zircon ages obtained from the Progress Granite (Zhao *et al.* 1992) represent a primary crystallization age, the D_2 is constrained to a structural episode that occurred ~ 550 Ma and D_3 to an episode younger or equal to 550 Ma. Zhao *et al.* (1993) obtained a $^{206}Pb/^{207}Pb$ apparent age of ~ 960 ± 6 Ma from four zircon separates from the Zhong Shan gneiss and argue that it is related to the syn-D_2 ~ 1000 Ma felsic intrusives in the Rauer Group. This suggests that the Zhong Shan orthogneiss intruded during a Neoproterozoic tectonothermal event, implying that the Larsemann Hills region was subsequently reworked during the Pan-African event, and the area was subjected to at least two major tectonothermal events.

If the Pan-African ages simply represent reset ages, then the real age of the major deformational events in the Larsemann Hills, D_2–D_3, and associated metamorphism is difficult to constrain. It is possible that D_2–D_3 represent the ~ 1000 Ma metamorphic event widely reported elsewhere in the East Antarctic Shield (e.g. Sheraton, Black & McCulloch, 1984). Supportive evidence for at least D_2 being of ~ 1000 Ma age, is the correlation of D_2 with pervasive deformation within the Rauer Group. As discussed above, the Rauer Group is dominated by thrust kinematics associated with south–southwest-plunging fold axes and pervasive lineation (D_6, Sims *et al.* 1994; D_{3-4}, Harley, 1987), that are co-linear with D_2 structures in the Larsemann Hills. Syn-D_2 felsic intrusives from the Rauer Group (Kinny, Black & Sheraton, 1993) indicate a Neoproterozoic age for pervasive D_2 deformation. If the regional correlation between D_2 in the Larsemann Hills and the Rauer Group is valid, then this strongly suggests D_2 in the Larsemann Hills is also Neoproterozoic (~ 1000 Ma) in age. Supporting this interpretation, the Zhong Shan gneiss, which intruded pre- to early syn-S_2 and records all episodes of D_2 deformation is dated at ~ 960 Ma ($^{206}Pb/^{207}Pb$ zircon, Zhao *et al.* 1993). An additional age constraint comes from Sm–Nd studies of peak metamorphic garnets in metabasites on Søstrene Island (~ 25 km west of the Larsemann Hills). These garnets are aligned in a lineation associated with thrusting that parallels L_{2x} (Dirks & Hand, 1994) and yields two point isochron ages of ~ 988 Ma (Hensen, pers. comm., 1994), further supporting a ~ 1000 Ma origin for D_2.

An additional possibility is that the extensional D_3 event is of Pan-African age (~ 550 Ma). The widespread occurrence of 'post-orogenic' voluminous granitoid bodies in the southern Prydz Bay area, often interpreted as Pan-African intrusives, and the common accepted view that many of the Pan-African ages obtained for this region represent a period of extensive resetting of isotopic systems, suggest a major regional thermal perturbation at ~ 550 Ma. It is unlikely that such a widespread high-grade thermal event associated with extensive felsic magmatic activity was unaccompanied by significant deformation (see, e.g. Sandiford *et al.* 1991), and given that the last major high-grade event in the region is D_3 suggests that this event may be the structural manifestation of the Pan-African thermal anomaly. The syn-D_3 nature of Landing Bluff granitoid bodies also supports a Pan-African age for D_3.

The age of D_4 is well constrained by the age of the planar pegmatites which are deformed by D_4 extensional mylonites. Similar planar pegmatites from the Rauer Group constrained to the Pan-African (500 ± 12 Ma, U–Pb SHRIMP techniques, Kinny, Black & Sheraton, 1993), provide a maximum age for D_4. These structures may represent the waning effects of the D_3 high-grade extension event.

7. Conclusions

The meta-sedimentary sequence of the Larsemann Hills preserves a workable stratigraphy that can be recognized throughout the area. Metabasite intercalations restricted to specific lithological units suggest a metavolcanic derivation, possibly in a mid-Pro-

terozoic extensional basin associated with volcanics. The opening of this basin may have coincided with an extensional event and the emplacement of voluminous dyke generations in the Vestfold Hills Archaean Block at 1370 and 1250 Ma (Dirks *et al.* 1993; Hoek, Dirks & Passchier, 1992; Lanyon, Black & Seitz, 1993), which is consistent with both Sm–Nd CHUR model ages of 1300–1600 Ma for most of these sediments in the Prydz Bay area (Sheraton, Black & McCulloch, 1984).

The high-grade structures in the Larsemann Hills can be subdivided in two groups, D_2 and D_3, each defined by a unique lineation direction and shear sense (Figs 3, 8). Each event is composite in nature and comprises high- and low-strain domains characterized by similar fold sequences. An important implication of this is that the gneissic layering in different parts of the Larsemann Hills did not necessarily develop all at the same time. S_3 dominated zones may have developed 500 Ma later than S_2 dominated zones, even though S_2 and S_3 appear identical in outcrop except for the mineral lineation direction they contain. The structural geometry of the Larsemann Hills is dominated by a major D_3 high-strain zone to the south, and a zone of diffuse D_3 reactivation to the north and with a low D_3 strain pocket in between, where S_2 structures are dominant. Assemblages in garnet–orthopyroxene–bearing tonalitic rocks record peak *P–T* conditions of ~ 7 kbar and ~ 780 °C early during D_2 followed by decompression and cooling to ~ 4.5 kbar at ~ 700 °C with progressive D_2 thrusting. During D_3 normal shearing, peak conditions may have been as high as 800 °C at ~ 4.5 kbar resulting in a second generation of re-equilibration textures and symplectites on remnant D_2 assemblages, mainly in aluminous pelites. During D_3 the growth of hydrous phases, especially biotite is important, as is the emplacement of a number of porphyritic granites.

To explain the Proterozoic decompression textures and the thermal regime prevailing in Prydz Bay, several workers have suggested tectonic models involving crustal thickening, delamination of the lower crust and subsequent extensional collapse (e.g. Fitzsimons & Harley, 1991; Thost, Hensen & Motoyoshi, 1991; Nichols & Berry, 1991) even though structural–kinematic data to prove or disprove these models are generally lacking. It is almost invariably assumed that this event occurred ~ 1000 Ma ago, whilst the 550 Ma events are equated with a passive thermal overprint and limited deformation (e.g. Stüwe & Powell, 1989*a*; Fitzsimons & Harley, 1991). Although our structural–kinematic data support a continuous D_2 thickening, D_3 extension thinning model, resulting in decompression textures, problems exist if one tries to match the structures with available age data. One possibility explored here is that D_2 and D_3 are separated by ~ 500 Ma. In this case, the superposition of two independent *P–T* loops, one at ~ 1000 Ma and a later one at slightly lower pressures at ~ 550 Ma, may give the appearance of a smooth retrograde *P–T* path (Dirks, Carson & Wilson, 1993). In fact it appears that most uplift in the Larsemann Hills occurred during D_2 and that decompression is a result of thrust-related uplift. D_3 may have been purely extensional in nature affecting a long since stabilized normal thickness crust.

Acknowledgements. We would like to extend thanks to all officers and expeditioners of the Australian National Antarctic Research Expeditions (ANARE) for assistance, co-operation and hospitality during the 1991/92 and 1992/93 field seasons. Logistic support by the Australian Antarctic Division and financial support from ASAC grant no. 519 are gratefully acknowledged. Many thanks to the expeditioners of both Zhong Shan Station (Peoples Republic of China) and Progress II (Commonwealth of Independent States) for their warm hospitality extended to us during our visits whilst in the Larsemann Hills. CJC and JPS acknowledge the receipt of Australian Post Graduate Research Awards. CJC gratefully acknowledges the financial assistance of the SOZ of the Netherlands and the use of department facilities and equipment whilst at the Faculty of Earth Sciences, University of Utrecht. We thank two anonymous referees for their comments which improved the text.

References

BHATTACHARYA, A., MOHANTY, L., MAJI, A., SEN, S. K. & RAITH, M. 1992. Non-ideal mixing in the phlogopite-annite binary: constraints from experimental data on Mg–Fe partitioning and a reformulation of the biotite-garnet geothermometer. *Contributions to Minearology and Petrology* **11**, 387–94.

BLACK, L. P., HARLEY, S. L., SUN, S. S. & MCCULLOCH, M. T. 1987. The Rayner complex of East Antarctica: complex isotopic systematics within a Proterozoic mobile belt. *Journal of Metamorphic Geology* **5**, 1–26.

CARSON, C. J., HAND, M. & DIRKS, P. H. G. M. 1995. Stable coexistence of grandidierite and kornerupine during medium pressure granulite facies metamorphism. *Mineralogical Magazine*. In press.

CLARKE, G. L. & POWELL, R. 1991. Decompressional coronas and symplectites in granulites of the Musgrave Complex, central Australia. *Journal of Metamorphic Geology* **9**, 441–50.

DIRKS, P. H. G. M., CARSON, C. J. & WILSON, C. J. L. 1993. The deformation history of the Larsemann Hills, Prydz Bay; the importance of the Pan-African (500 Ma) in East Antarctica. *Antarctic Science* **5**, 179–92.

DIRKS, P. H. G. M. & HAND, M. 1995. Clarifying temperature-pressure paths via structures in granulite from the Bolingen Islands, Antarctica. *Australian Journal of Earth Sciences*. In press.

DIRKS, P. H. G. M., HOEK, J. D., WILSON, C. J. L. & SIMS, J. P. 1993. The Proterozoic deformation of the Vestfold Hills, East Antarctica: implications for the tectonic development of adjacent granulite belts. *Precambrian Research* **65**, 277–95.

FITZSIMONS, I. C. W. & HARLEY, S. L. 1991. Geological relationships in high-grade gneiss of the Brattstrand

Bluffs coastline, Prydz Bay, east Antarctica. *Australian Journal of Earth Sciences* **38**, 497–519.

FITZSIMONS, I. C. W. & HARLEY, S. L. 1992. Mineral reaction textures in high-grade gneisses: evidence for contrasting pressure-temperature paths in the Proterozoic Complex of East Antarctica. In *Recent Progress in Antarctic Earth Science* (eds Y. Yoshida, K. Kaminuma and K. Shiraishi), pp. 103–11. Tokyo: Terra Scientific Publishing.

GANGULY, J. & SAXENA, S. K. 1984. Mixing properties of aluminosilicate garnets: constraints from natural and experimental data and application to geothermobarometry. *American Mineralogist* **69**, 88–97.

GRANT, J. A. 1985. Phase equilibria in partial melting of pelitic rocks. In *Migmatites* (ed. J. R. Ashworth), pp. 86–144. London: Blackie.

HARLEY, S. L. 1984*a*. The solubility of alumina in orthopyroxene coexisting with garnet in FeO–MgO–Al_2O_3–SiO_2 and CaO–FeO–MgO–Al_2O_3–SiO_2. *Journal of Petrology* **25**, 665–96.

HARLEY, S. L. 1984*b*. An experimental study of the partitioning of Fe and Mg between garnet and orthopyroxene. *Contributions to Mineralogy and Petrology* **86**, 359–73.

HARLEY, S. L. 1987. Precambrian geological relationships in high-grade gneisses of the Rauer Islands, East Antarctica. *Australian Journal of Earth Sciences* **34**, 175–207.

HARLEY, S. L. 1988. Proterozoic granulites from the Rauer Group, East Antarctica. I. Decompressional pressure–temperature Paths deduced from mafic and felsic gneisses. *Journal of Petrology* **29**, 1059–95.

HARLEY, S. L. & FITZSIMONS, I. C. W. 1991. Pressure–temperature evolution of metapelitic granulites in a polymetamorphic terrane: The Rauer Group, East Antarctica. *Journal of Metamorphic Geology* **9**, 231–43.

HARLEY, S. L., FITZSIMONS, I. C. W., BUICK, I. S. & WATT, G. 1992. The significance of reworking, fluids and partial melting in granulite metamorphism, East Prydz Bay, Antarctica. In *Recent Progress in Antarctic Earth Science* (ed. Y. Yoshida, K. Kaminuma and K. Shiraishi), pp. 103–11. Tokyo: Terra Scientific Publishing.

HARLEY, S. L. & GREEN, D. H. 1982. Garnet-orthopyroxene barometry for granulites and peridotites. *Nature* **300**, 697–701.

HOEK, J. D., DIRKS, P. H. G. M. & PASSCHIER, C. W. 1992. A late-Proterozoic extensional–compressional tectonic cycle in East Antarctica. In *Recent Progress in Antarctic Earth Sciences* (eds Y. Yoshida, K. Kaminuma and K. Shiraishi), pp. 137–43. Tokyo: Terra Scientific Publishing.

KINNY, P. D., BLACK, L. P. & SHERATON, J. W. 1993. Zircon ages and the distribution of Archean and Proterozoic rocks in the Rauer Islands. *Antarctic Science* **5**, 193–206.

KOBER, B. 1986. Whole-grain evaporation for $^{207}Pb/^{206}Pb$ age investigations on single zircons using a double-filament thermal ion source. *Contributions to Mineralogy and Petrology* **93**, 482–90.

KOBER, B. 1987. Single-zircon evaporation combined with Pb+ emitter bedding for $^{207}Pb/^{206}Pb$-age investigations using thermal ion mass spectrometry, and implications to zirconology. *Contributions to Mineralogy and Petrology* **96**, 63–71.

LANYON, R., BLACK, L. P. & SEITZ, H.-M. 1993. U–Pb zircon dating of mafic dykes and its application to the Proterozoic geological history of the Vestfold Hills, East Antarctica. *Contributions to Mineralogy and Petrology* **115**, 184–203.

MEZGER, K., ESSENE, E. J. & HALLIDAY, A. N. 1992. Closure temperatures of the Sm–Nd sysdtem in metamorphic garnets. *Transactions of the American Geophysical Union EOS* **73**, 373.

MOTOYOSHI, Y., THOST, D. E. & HENSEN, B. J. 1991. Reaction textures in calc-silicate granulites from the Bolinger Islands, Prydz Bay, Antarctica: implications for the retrograde *P–T* path. *Journal of Metamorphic Geology* **9**, 293–300.

NEWTON, R. C. & PERKINS III, D. 1982. Thermodynamic calibration of geobarometers based on the assemblages garnet-plagioclase-orthopyroxene (clinopyroxene)-quartz. *American Mineralogist* **67**, 203–22.

NICOLS, G. T. & BERRY, R. F. 1991. A decompressional *P–T* path, Reinbolt Hills, East Antarctica. *Journal of Metamorphic Geology* **9**, 257–66.

PLATT, J. P. & VISSERS, R. L. 1980. Extensional structures in anisotropic rocks. *Journal of Structural Geology* **2**, 397–410.

POWELL, R. & HOLLAND, T. J. B. 1994. Optimal geothermometry and geobarometry. *American Mineralogist* **79**, 120–33.

REN, L., ZHAO, Y., LIU, X. & CHEN, T. 1992. Re-examination of the metamorphic evolution of the Larsemann Hills, East Antarctica. In *Recent Progress in Antarctic Earth Sciences* (eds Y. Yoshida, K. Kaminuma and K. Shiraishi), pp. 145–53. Tokyo: Terra Scientific Publishing.

SANDIFORD, M., MARTIN, N., ZHOU, S. & FRASER, G. 1991. Mechanical consequences of granite emplacement during high-T, low-P metamorphism and the origin of 'anticlockwise' *P–T* paths. *Earth and Planetary Science Letters* **107**, 164–72.

SEN, S. K. & BHATTACHARYA, A. 1984. An orthopyroxene-garnet thermometer and its application to the Madras charnockites. *Contributions to Mineralogy and Petrology* **88**, 64–71.

SHERATON, J. W., BLACK, L. P. & MCCULLOCH, M. T. 1984. Regional geochemical and isotopic characteristics of high-grade metamorphics of the Prydz Bay area: the extent of Proterzoic reworking of Archaean continental crust in East Antarctica. *Precambrian Research* **26**, 169–98.

SIMS, J. P., DIRKS, P. H. G. M., CARSON, C. J. & WILSON, C. J. L. 1994. The structural evolution of the Rauer Group, East Antarctica; mafic dykes as passive markers in a composite Proterzoic terrain. *Antarctic Science* **6**, 379–94.

STÜWE, K., BRAUN, H. M. & PEER, H. 1989. Geology and structure of the Larsemann Hills area, East Antarctica. *Australian Journal of Earth Sciences* **36**, 219–41.

STÜWE, K. & POWELL, R. 1989*a*. Low pressure granulite facies metamorphism in the Larsemann Hills area, East Antarctica; petrology and tectonic implications for the Prydz Bay area. *Journal of Metamorphic Geology* **7**, 465–84.

STÜWE, K. & POWELL, R. 1989*b*. Metamorphic segregations associated with garnet and orthopyroxene porphyroblast growth: two examples from the Larsemann Hills, East Antarctica. *Contributions to Mineralogy and Petrology* **103**, 523–30.

THOST, D. E., HENSEN, B. J. & MOTOYOSHI, Y. 1991. Two-

stage decompression in garnet-bearing mafic granulites from Sostrene Island, Prydz Bay, East Antarctica. *Journal of Metamorphic Geology* **9**, 293–300.

THOST, D. E., MOTOYOSHI, Y. & HENSEN, B. J. 1988. Low pressure granulite metamorphism in the Bolingen Islands, East Antarctica. *Terra Cognita* **8**, 247.

TINGEY, R. J. 1981. Geological investigations in Antarctica 1968–1969: the Prydz Bay–Amery ice Shelf–Prince Charles Mountains area. *Bureau of Mineral Resources, Australia, Record*, 1981/34.

ZHAO, Y., LI, J., LIU, X., SONG, B., ZHANG, Z., FU, Y., CHEN, T., WANG, Y., REN, L. & YAO, Y. 1993. Early Palaeozoic (Pan-African) thermal event of the Larsemann Hills and its neighbours, Prydz Bay, East Antarctica (abstr.). In *The Tectonics of East Antarctica*, Conference Abstracts, Utrecht, 1993.

ZHAO, Y., SONG, B., WANG, Y., REN, L., LI, J. & CHEN, T. 1992. Geochronology of the late granite in the Larsemann Hills, East Antarctica. In *Recent Progress in Antarctic Earth Science* (eds Y. Yoshida, K. Kaminuma and K. Shiraishi), pp. 155–61. Tokyo: Terra Scientific Publishing.